Structural Analysis
Part III - X-ray tools

Session 4:

X-ray diffraction applications
X-ray spectroscopy

Reminder about previous weeks

Atomic scattering factors again

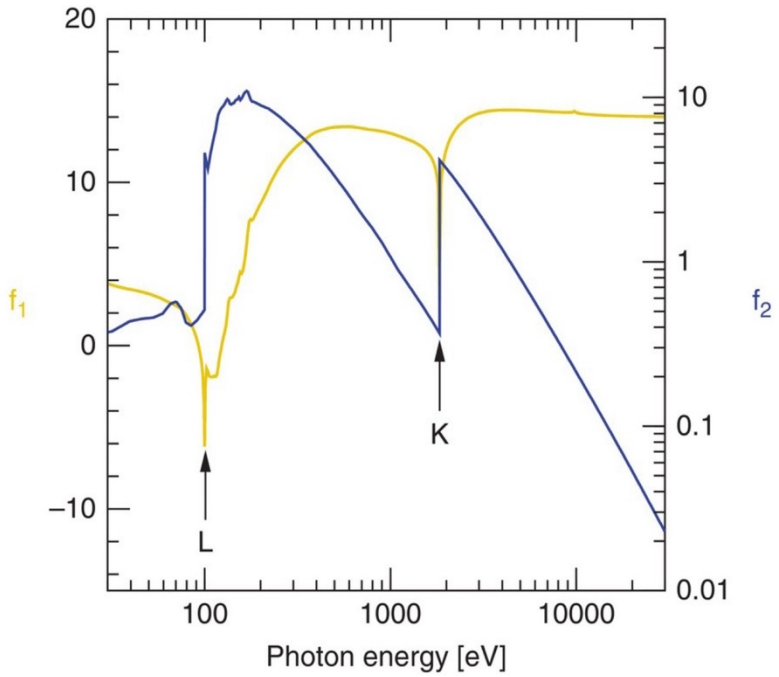

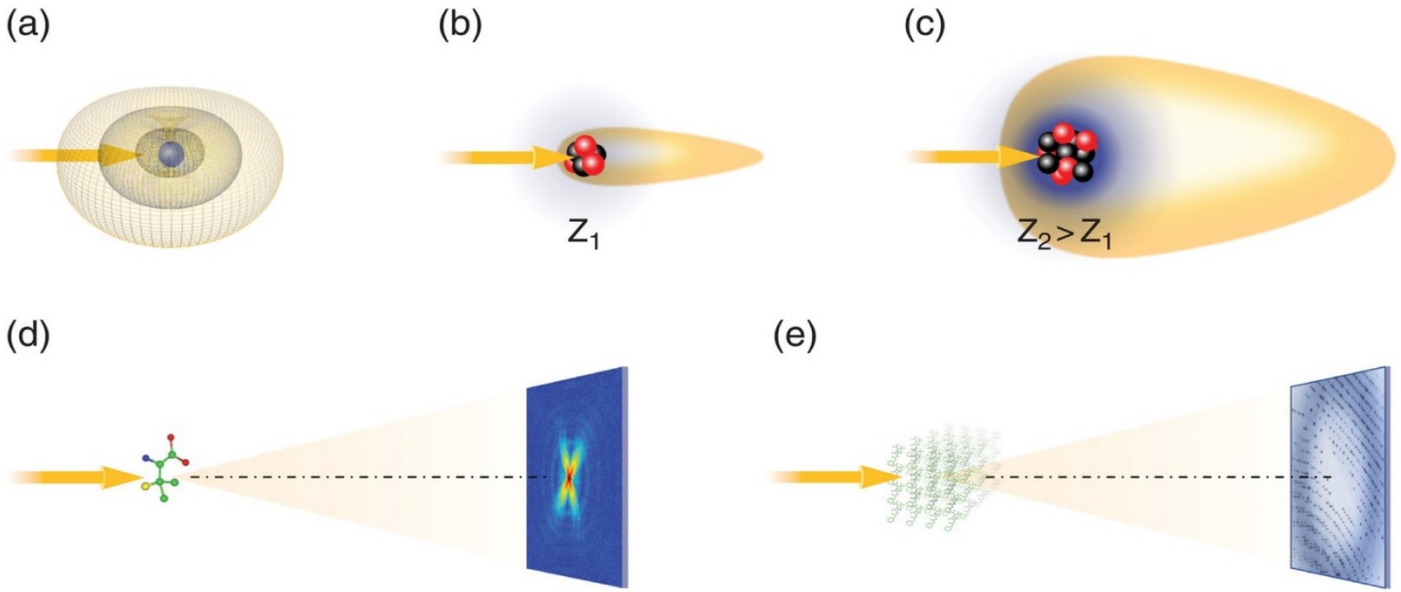

$f \to 0$ for $Q \to \infty$

$$f(Q, h\nu) = f^{\circ}(Q) + f'(h\nu) + i f''(h\nu)$$

"scattering" absorption

For each lattice a reciprocal lattice can be defined

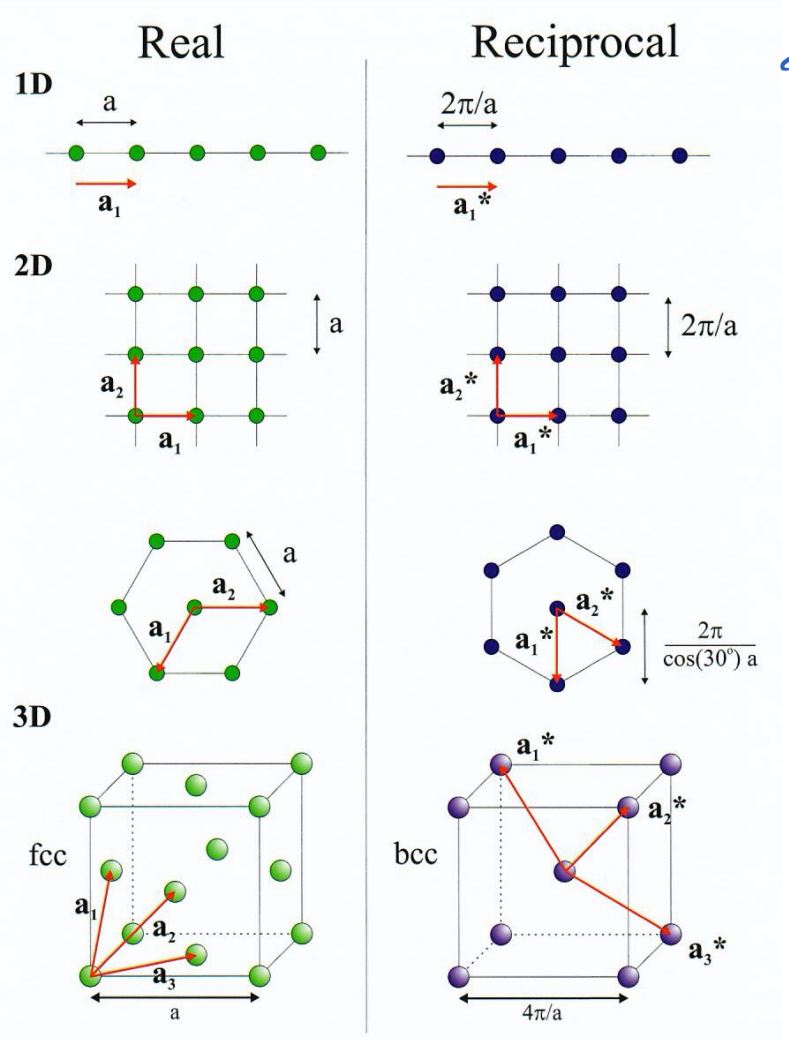

→ For each Lattice there exists a so called reciprocal Lattice

→ The reciprocal Lattice is the Fourier Transform of the direct Lattice

→ Reciprocal Lattices is defined by

$$\vec{G} = h\vec{a}_1^* + k\vec{a}_2^* + l\vec{a}_3^*$$

$$|\vec{G}| = \frac{2\pi}{d_{hkl}}$$

$\vec{G}$ perpendicular on planes

hkl → Miller indices

Bargg and Laue conditions

Real Reciprocal

(a) Equivalence of Bragg and Laue

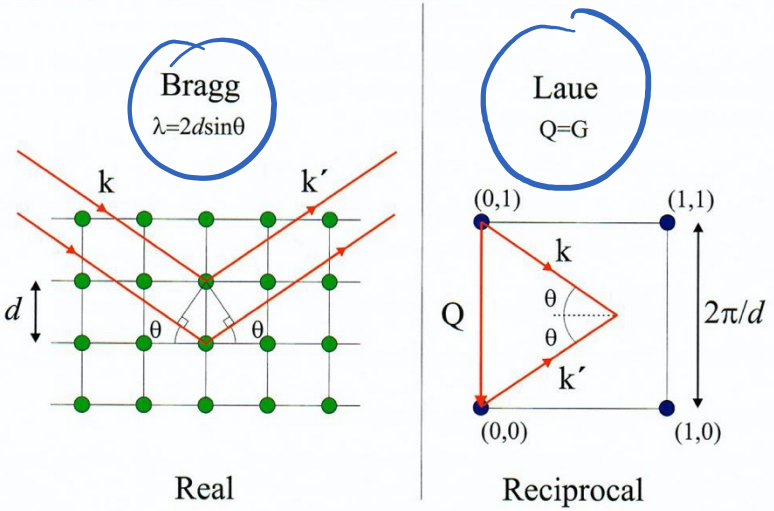

(b) Miller indices and reciprocal lattice vectors

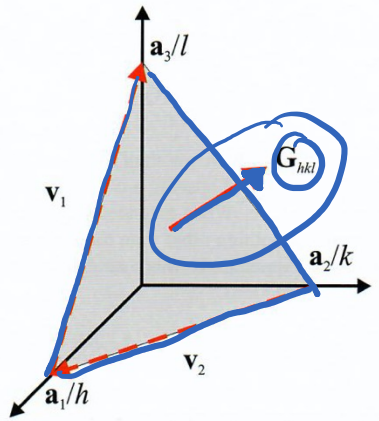

The Nobel Prize in Physics 1914

Photo from the Nobel Foundation archive.
Max von Laue
Prize share: 1/1

In reciprocal space one can show that constructive interference is obtained for

$$\vec{Q} = \vec{G}$$

$\vec{G}$ → perpendicular to the planes with Miller indices h, k, l

$|\vec{G}| = \frac{2\pi}{d_{hkl}}$ ⇒ Lattice spacing of hkl planes

The Ewald Sphere

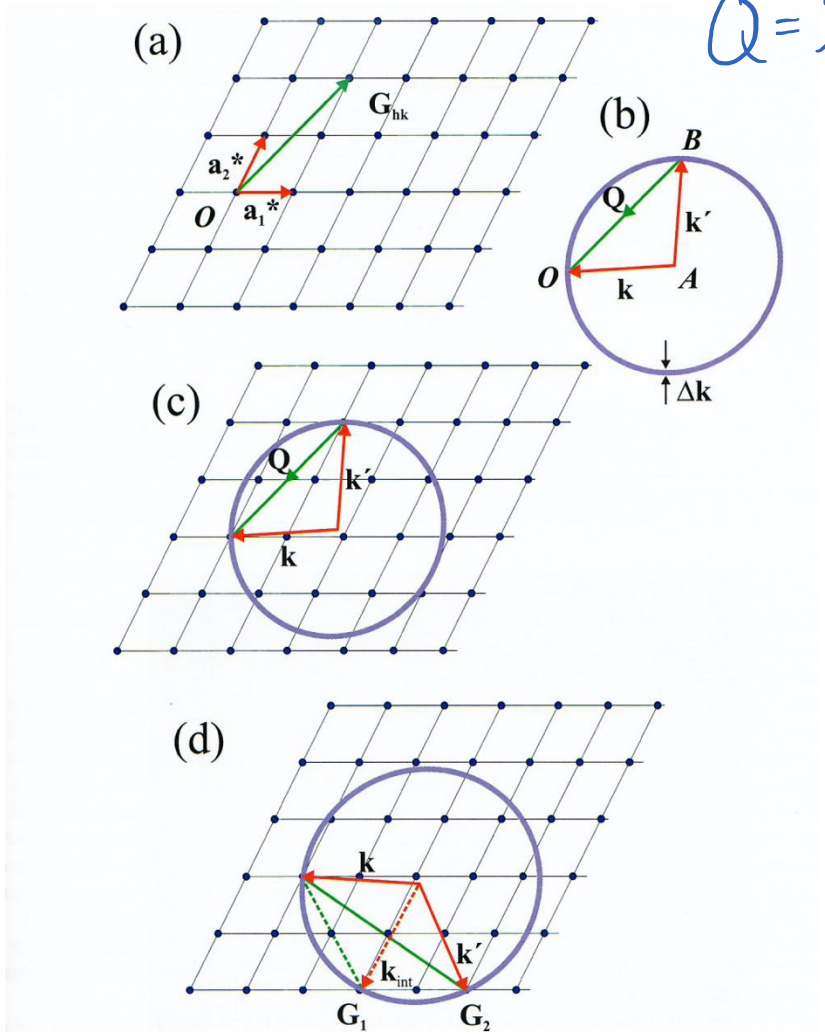

- Elegant geometric construction of relationship

$\vec{Q} = \vec{k} - \vec{k}'$ → wave vector $\vec{k}$

→ diffraction angle

→ in reciprocal lattice

- Laue condition $\vec{Q} = \vec{G}_{hkl}$

- Create sphere with radius $\vec{k}$ (circle in 2D)

- Move sphere at origin O

- Monochromatic light can be scattered constructively ("signal") whenever sphere overlaps with reciprocal lattice point as here $\vec{Q} = \vec{G}$

More on Bragg peaks

A crystal is defined by ist lattice and basis

unit cell + translational symmetry ⇒ Lattice

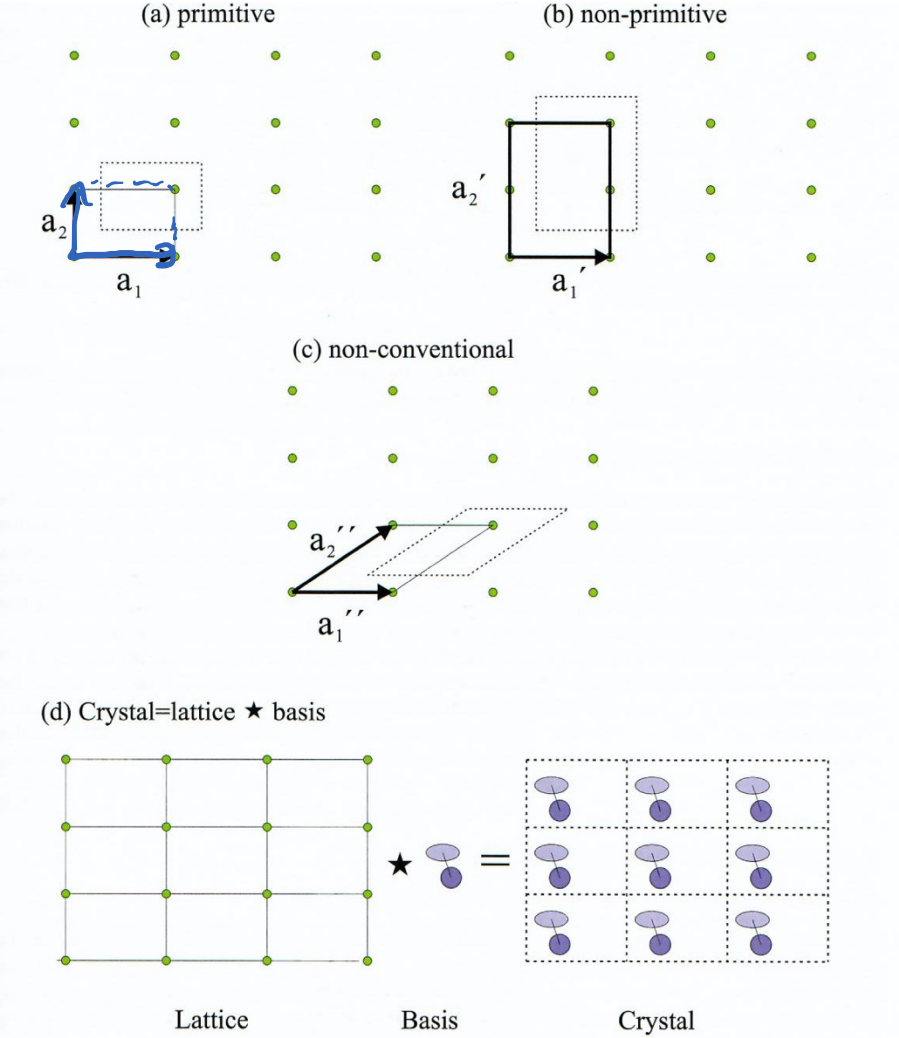

$$\text{Crystal } C(x) = \sum_n B(x-n)$$

(Base)

$$\text{Lattice } \mathcal{L}(x) = \sum \delta(x-n)$$

$$C(x) = \mathcal{L}(x) \otimes B(x)$$

or in plain English

Crystal = Lattice ⊗ Base

The structure factor

box ⊗ Lattice = Crystal

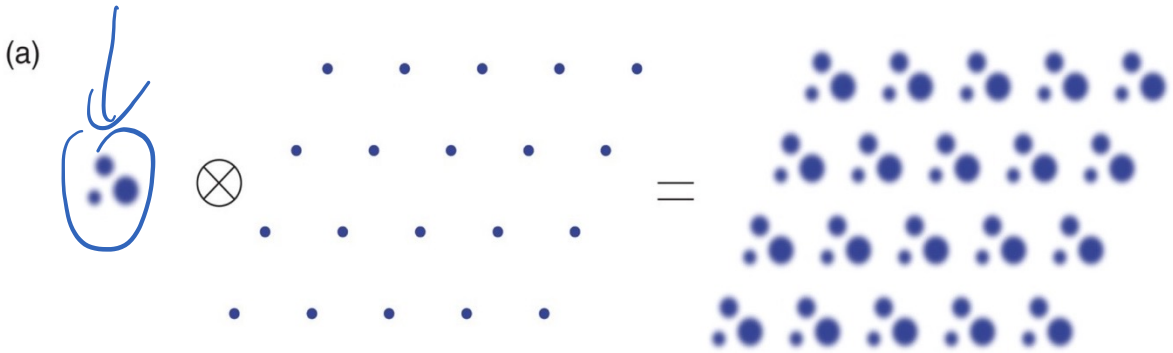

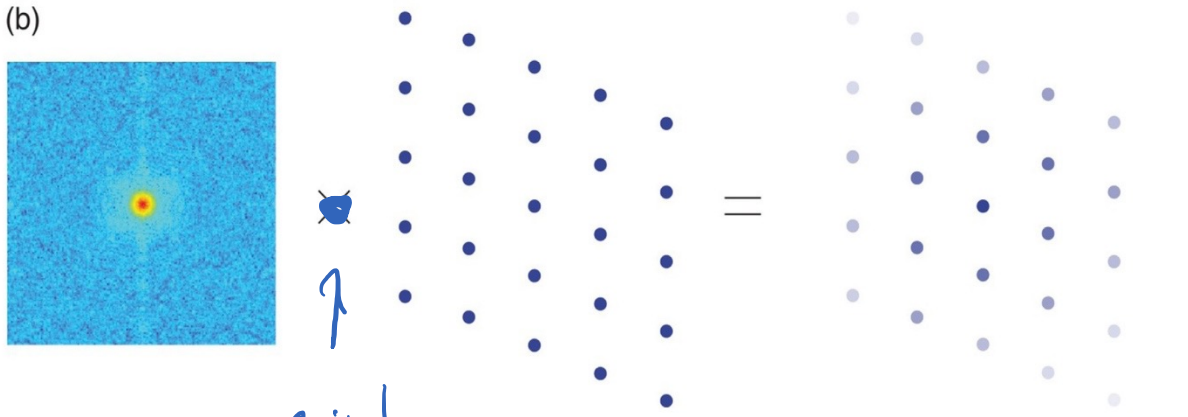

FT(box) point product FT(Lattice) = FT(crystal)

Decomposition of scattering

$$F_{(Q)}^{\text{crystal}} = \sum_{\text{atoms}} f_{e(Q)}\, e^{iQr}$$

↓ leave | to physicists

$$F_{\text{crystal}} = \underbrace{\sum e^{iQR_n}}_{\text{Lattice}} \underbrace{\sum f_i(Q)\, e^{iQr}}_{\text{Base}}$$

Lattice: geometry info | Base: structure factor

Other way of saying this:
Crystal in real space = convolution Lattice ⊗ Base
in diffraction FT(Lattice) • FT(Base)

The structure factor

→ incoming X-rays scatter atoms #1-3

→ how does relative position reflect on Bragg interference

→ We need to consider amplitude & phase

⇒ Defines structure factor

$$F_{hkl} = \sum_i f_i \exp[-i2\pi(hx_i + ky_i + lz_i)]$$

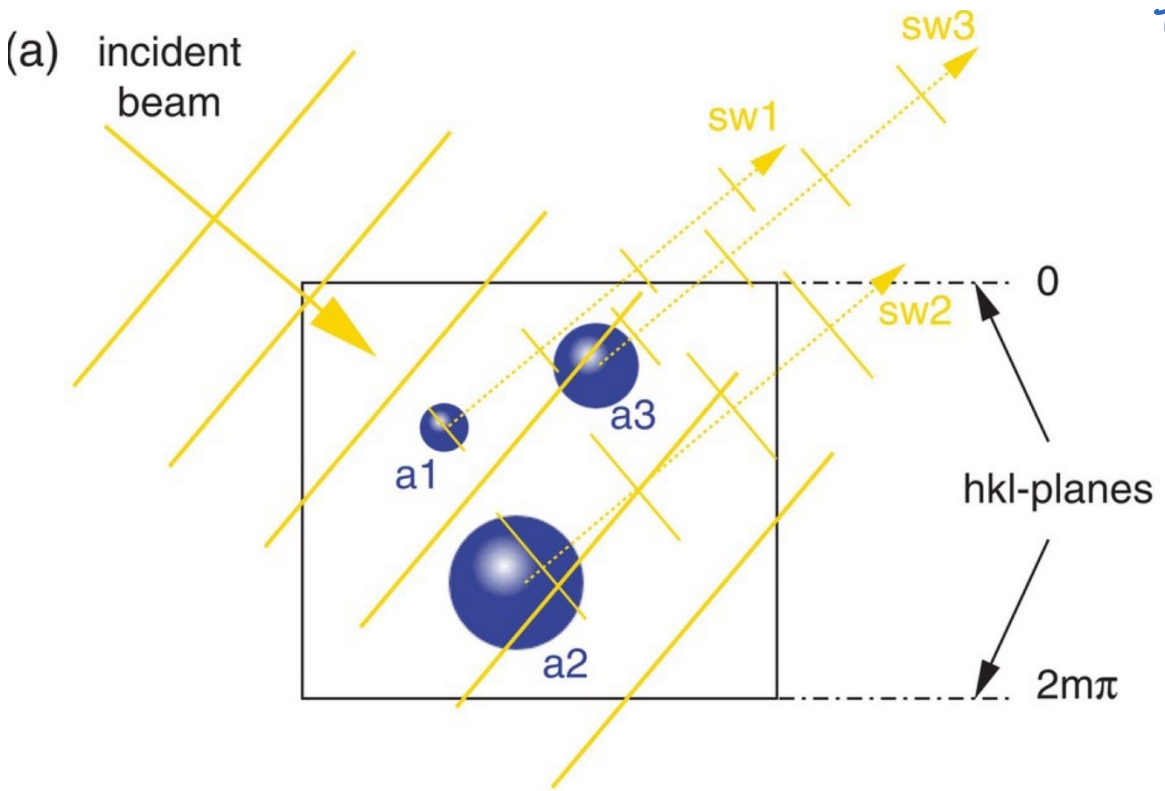

(b)

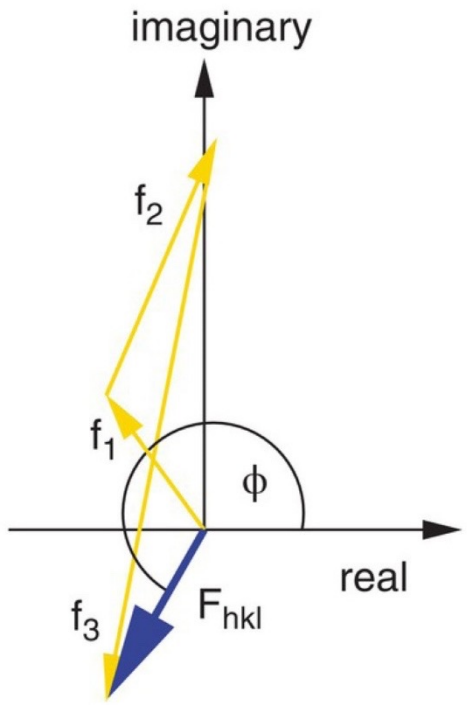

Allowed and forbidden reflections

→ There exists systematic absences due to the symmetry of the unit cell

→ "forbidden reflections"

→ can help classify the Lattice

all allowed

h+k+l = odd are missing

odd/even mixed missing

most complicated

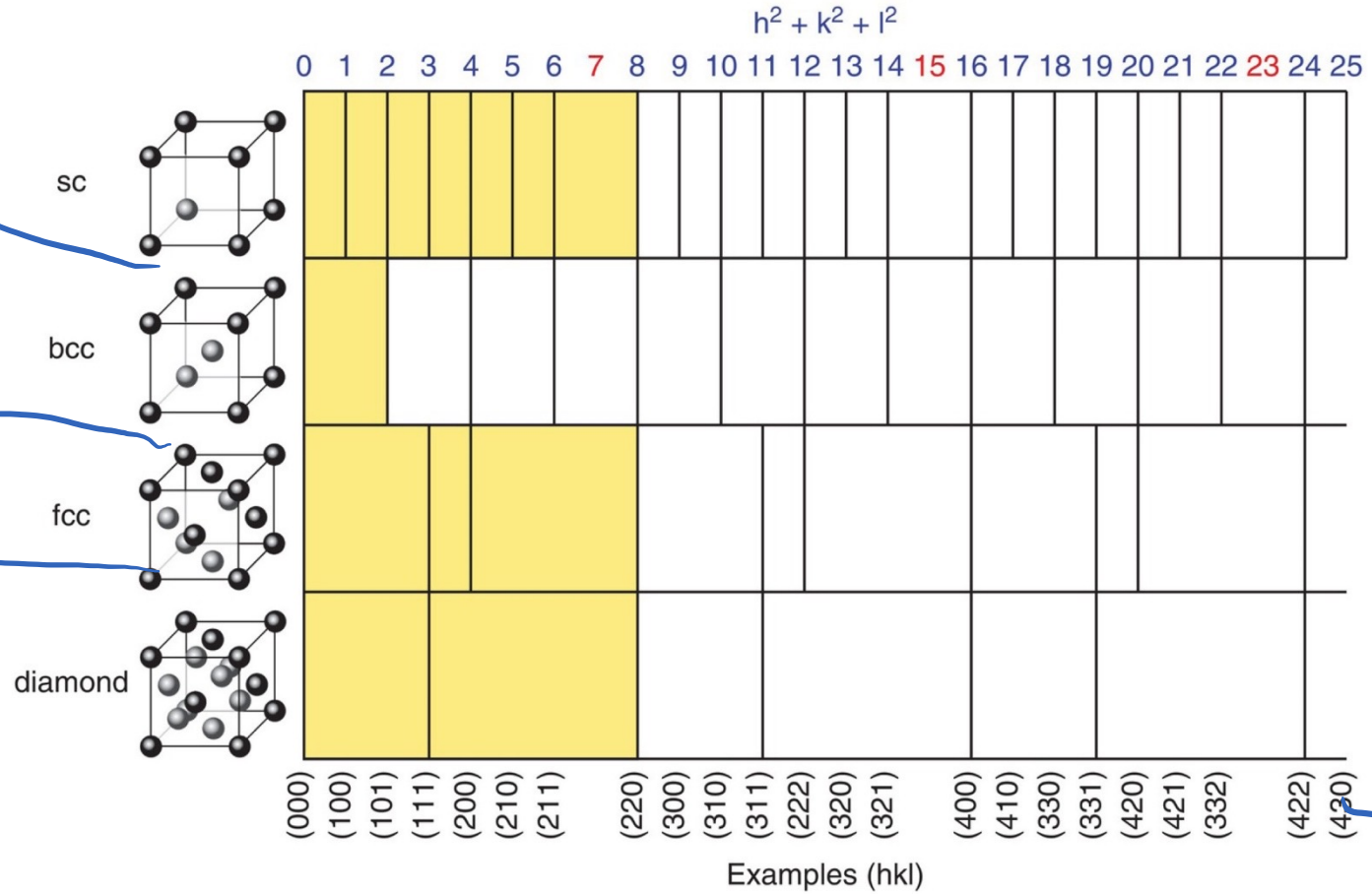

highlights shortcomings of simple Bragg law

↓

not just reflections we are talking about

but it requires detailed knowledge of scattering strengths positions

Friedels law

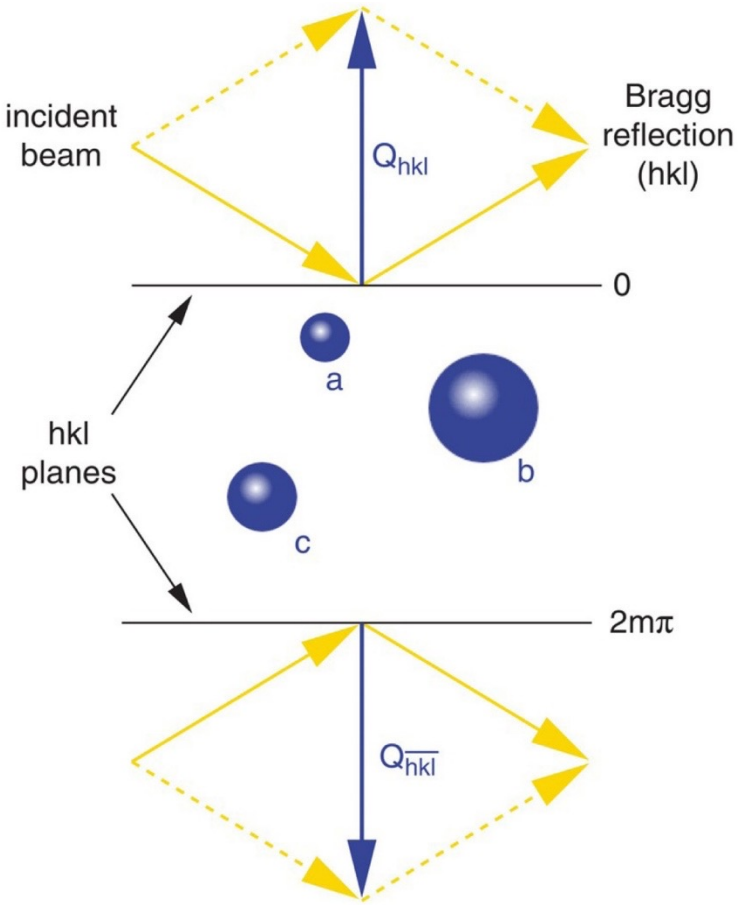

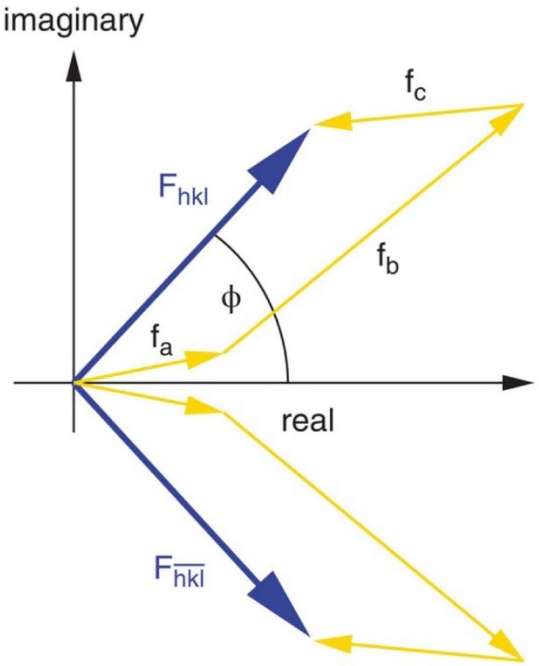

The phase problem

Problem

→ calculation of X-ray diffraction pattern is easy
→ FT

→ but we need to do inverse problem

$$\rho(Q) = FT(\rho(r))$$

$$FT^{-1}\rho(Q) = \rho(r)$$

↳ we need phase

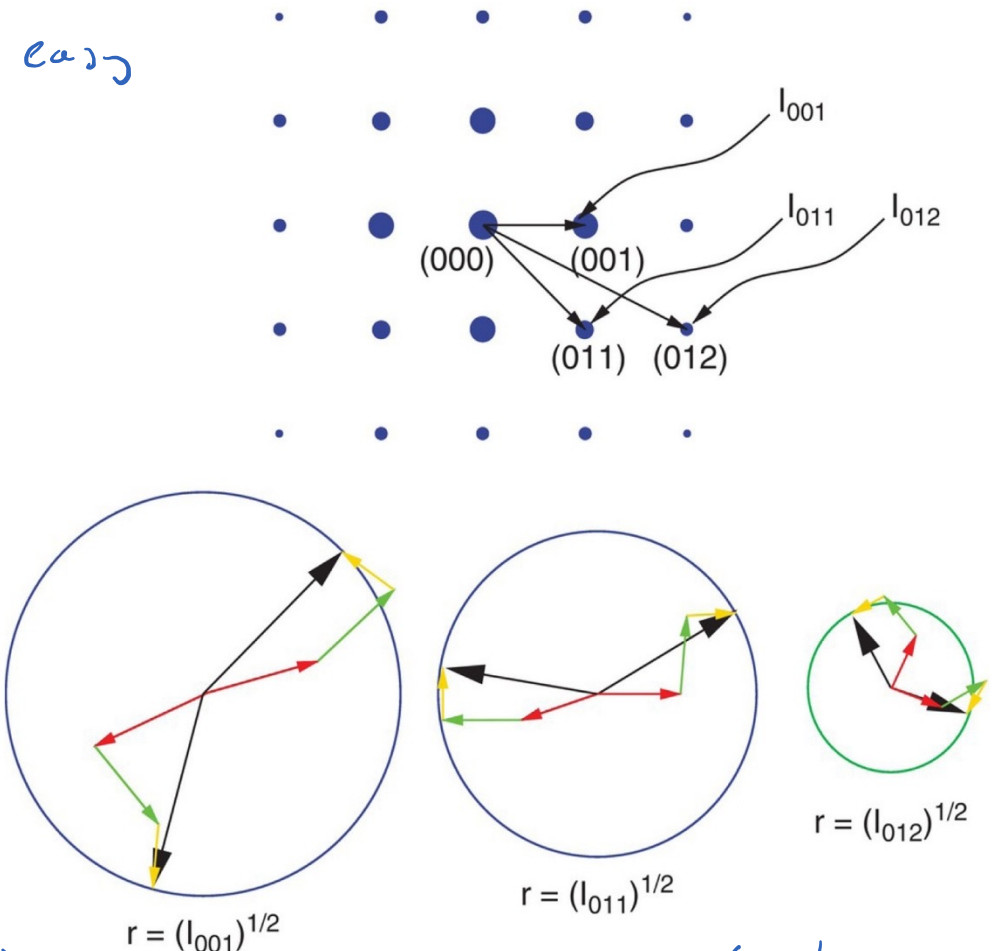

→ But ...

we measure intensities $I = |A|^2$ → phase lost

Solving a crystal structure

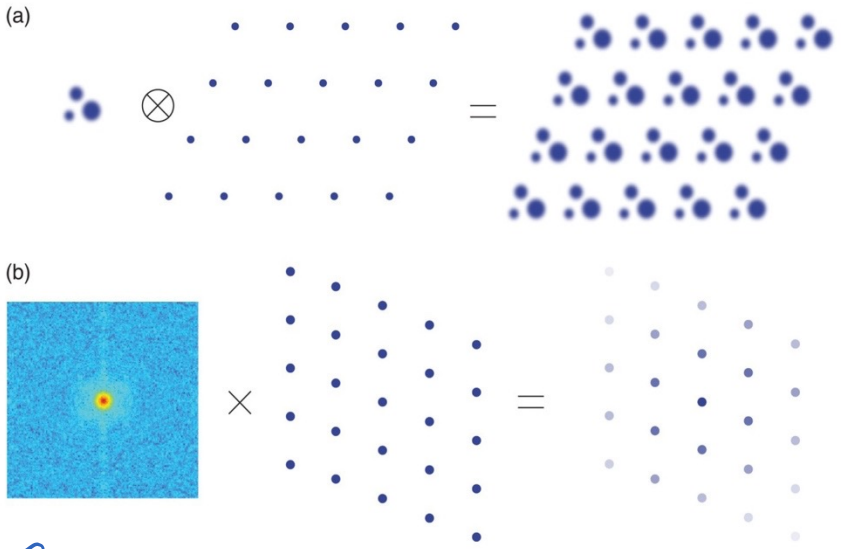

Solution

- Over measure problem
- measure more reflections than needed to reconstruct unit cell
- Bragg spots intensities – structure factor amp

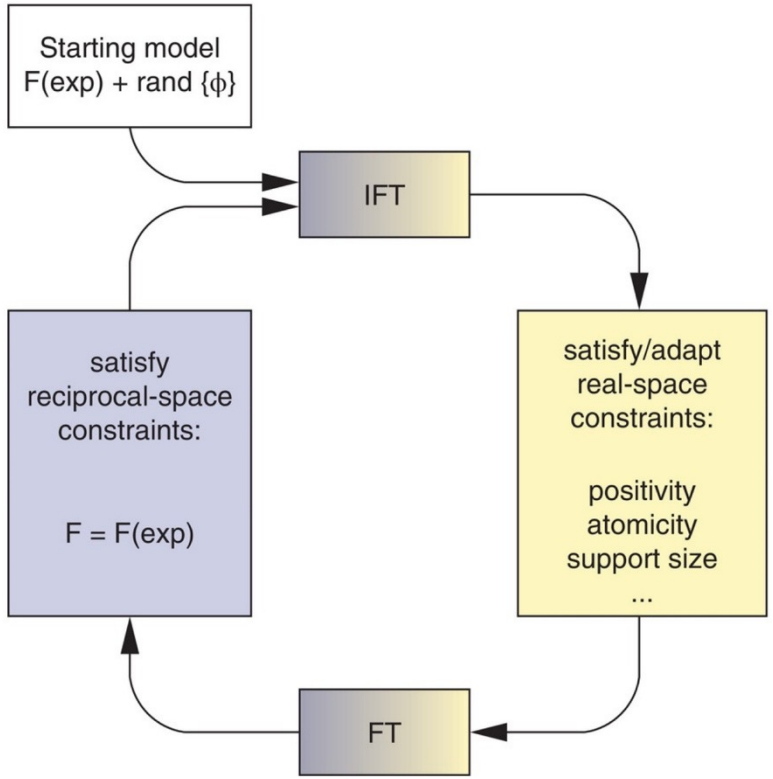

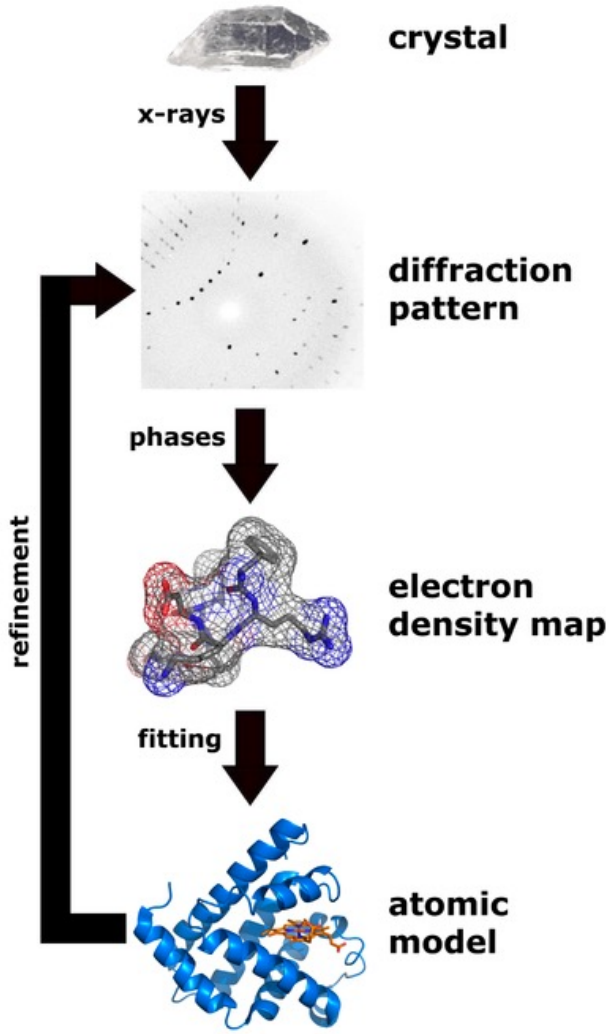

A few examples and case studies

Remember last week example for diffaction of lysozyme crystal

Lysozym (Protein, Immunsystem)

Stochiometric formula

$C_{125}H_{196}N_{40}O_{36}S_2$

Structure

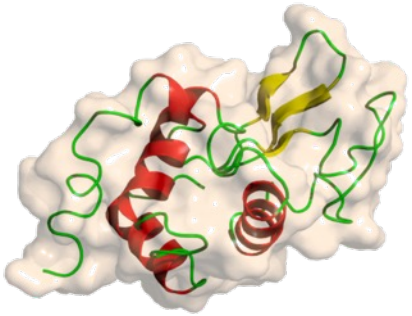

Crystal

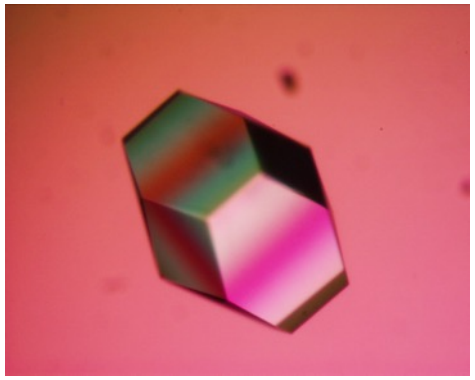

Experiment at the Swiss Light Source

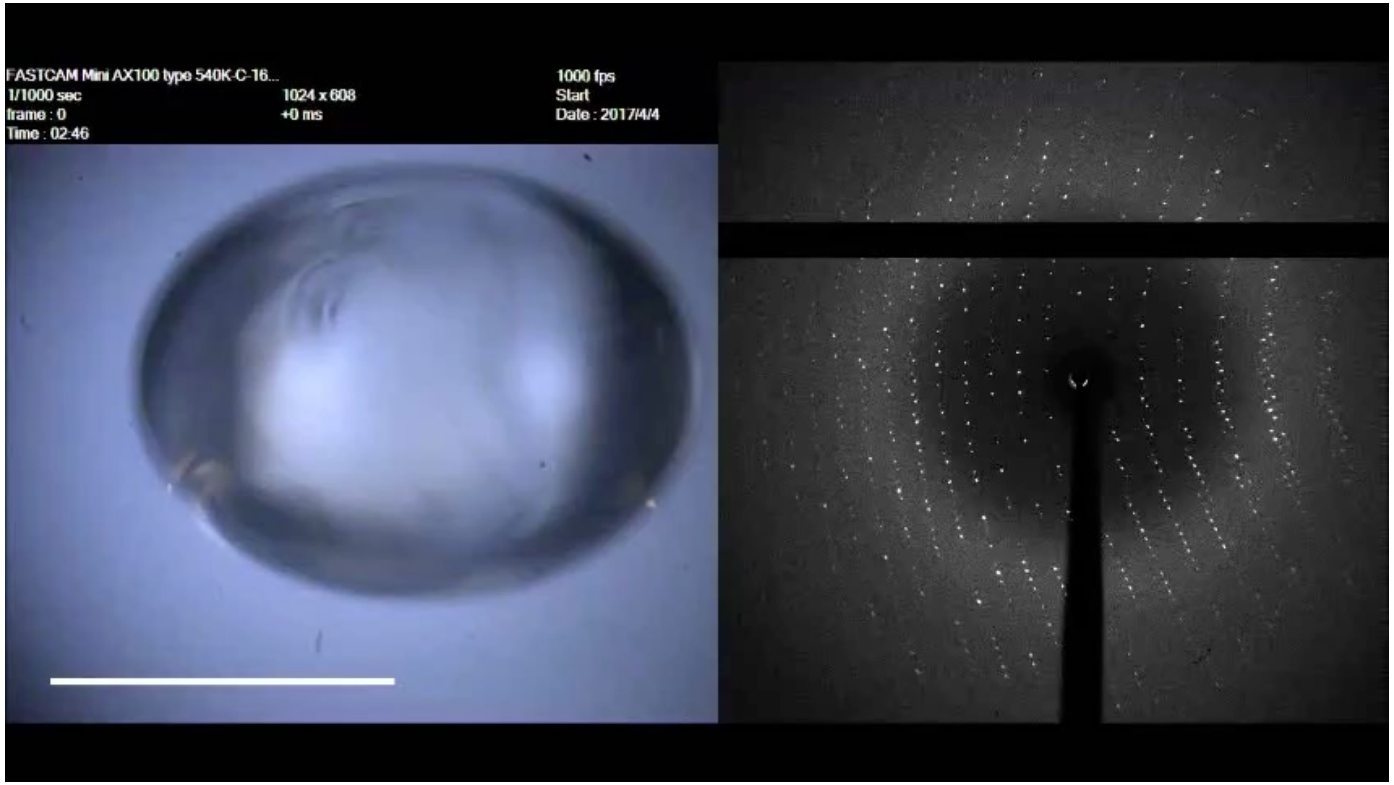

Each X-ray source allows characteristic experiments. „Output“ varies by >20 orders of magnitude

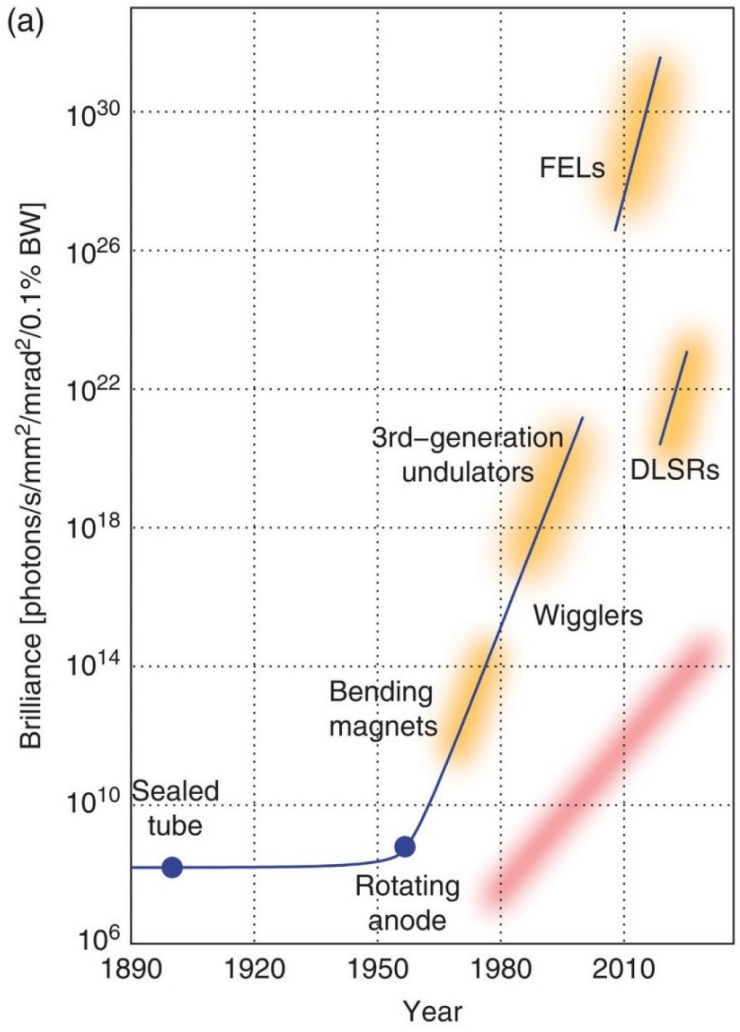

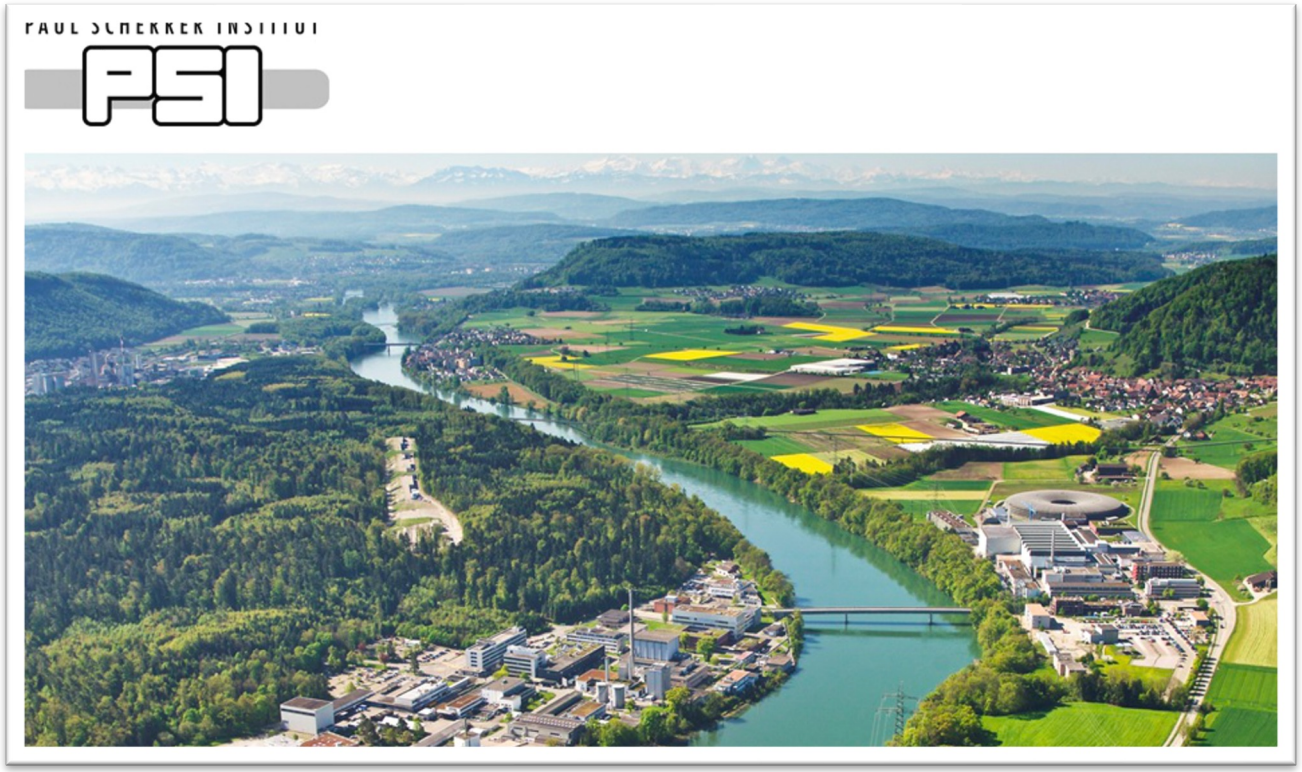

X-ray diffraction patterns from micro (nano) crystals

Science 337, page 363 (2012)

High-Resolution Protein Structure Determination by Serial Femtosecond Crystallography

Sébastien Boutet,[1]* Lukas Lomb,[2,3] Garth J. Williams,[1] Thomas R. M. Barends,[2,3] Andrew Aquila,[4] R. Bruce Doak,[5] Uwe Weierstall,[5] Daniel P. DePonte,[4] Jan Steinbrener,[2,3] Robert L. Shoeman,[2,3] Marc Messerschmidt,[1] Anton Barty,[4] Thomas A. White,[4] Stephan Kassemeyer,[2,3] Richard A. Kirian,[5] M. Marvin Seibert,[1] Paul A. Montanez,[1] Chris Kenney,[6] Ryan Herbst,[6] Philip Hart,[6] Jack Pines,[6] Gunther Haller,[6] Sol M. Gruner,[7,8] Hugh T. Philipp,[7] Mark W. Tate,[7] Marianne Hromalik,[9] Lucas J. Koerner,[10] Niels van Bakel,[11] John Morse,[12] Wilfred Ghonsalves,[1] David Arnlund,[13] Michael J. Bogan,[14] Carl Caleman,[4] Raimund Fromme,[15] Christina Y. Hampton,[14] Mark S. Hunter,[15] Linda C. Johansson,[13] Gergely Katona,[13] Christopher Kupitz,[15] Mengning Liang,[4] Andrew V. Martin,[4] Karol Nass,[16] Lars Redecke,[17,18] Francesco Stellato,[4] Nicusor Timneanu,[19] Dingjie Wang,[5] Nadia A. Zatsepin,[5] Donald Schafer,[1] James Defever,[1] Richard Neutze,[13] Petra Fromme,[15] John C. H. Spence,[5] Henry N. Chapman,[4,16] Ilme Schlichting[2,3]

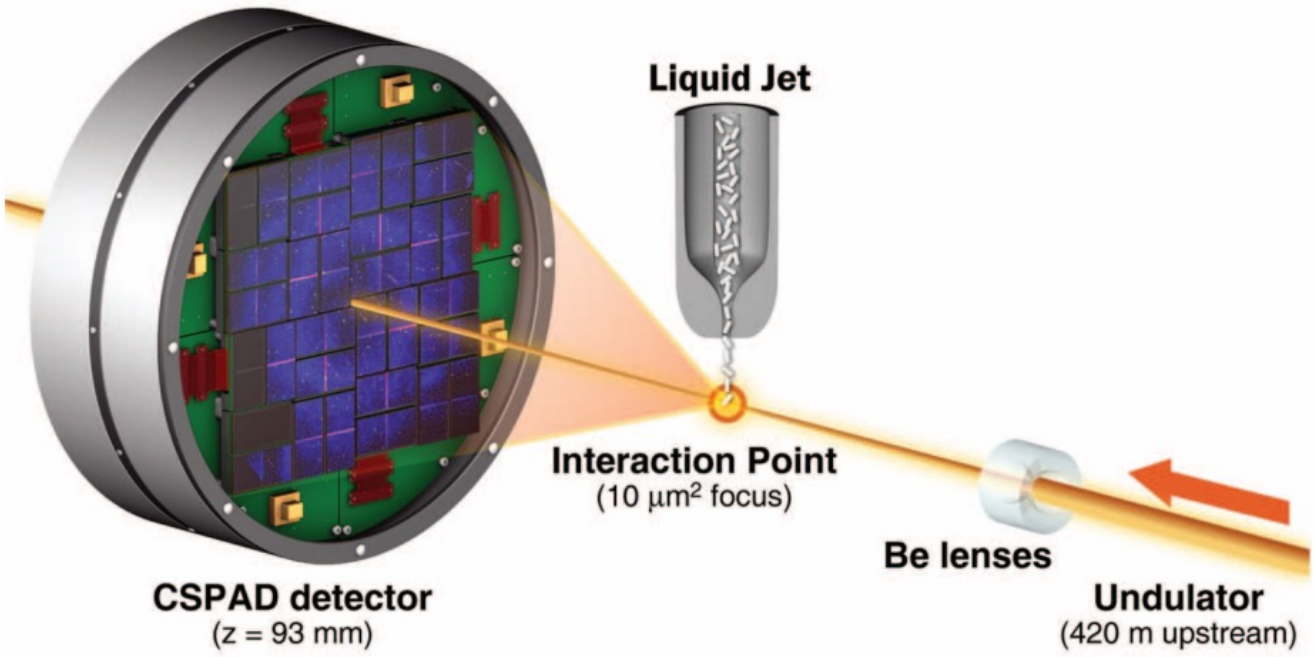

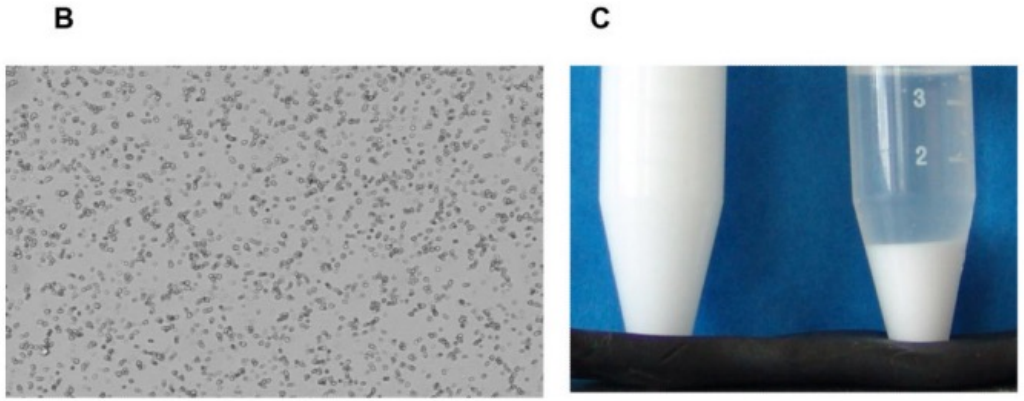

Time-resolved x-ray diffraction

nature

Letter | Published: 09 July 2014

Serial time-resolved crystallography of photosystem II using a femtosecond X-ray laser

Christopher Kupitz, Shibom Basu, [...] Petra Fro

Nature **513**, 261–265(2014) | Cite this article

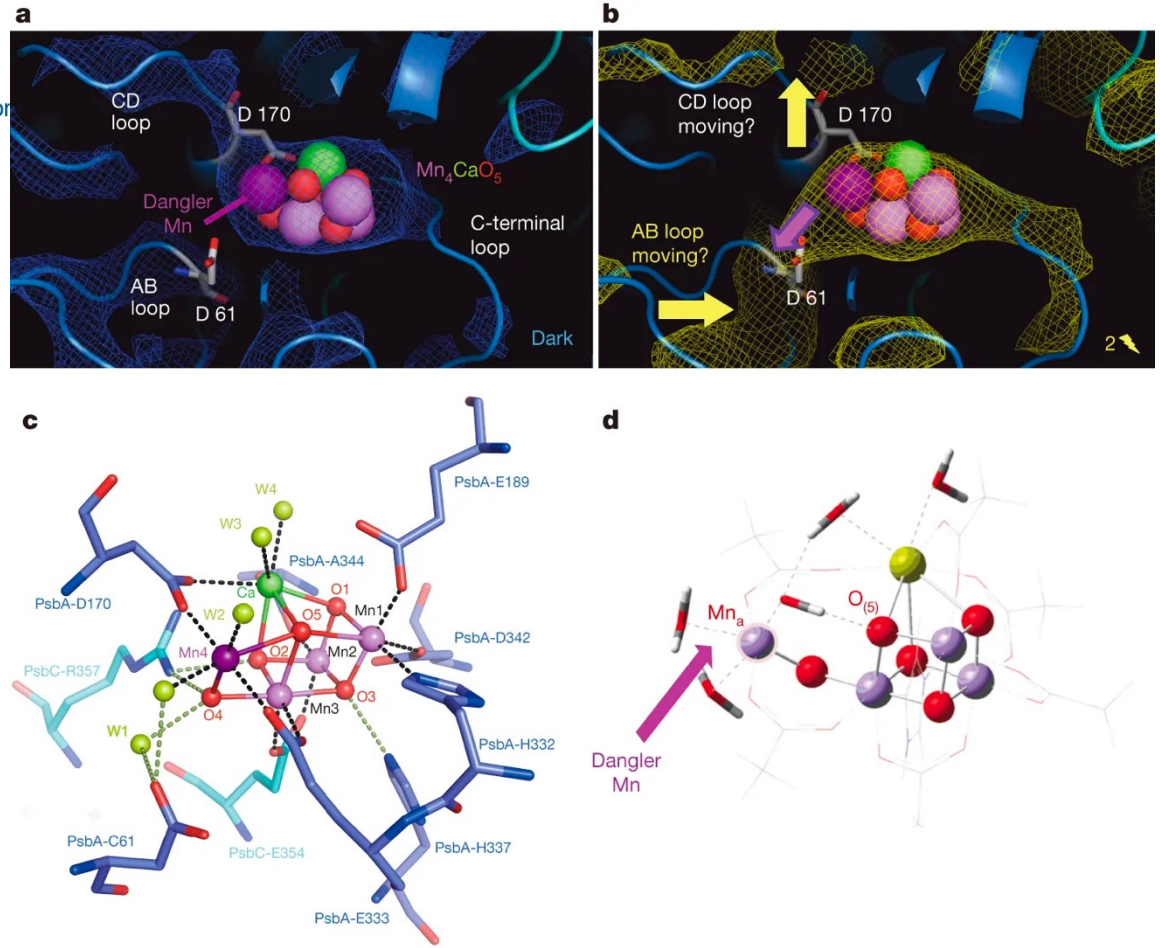

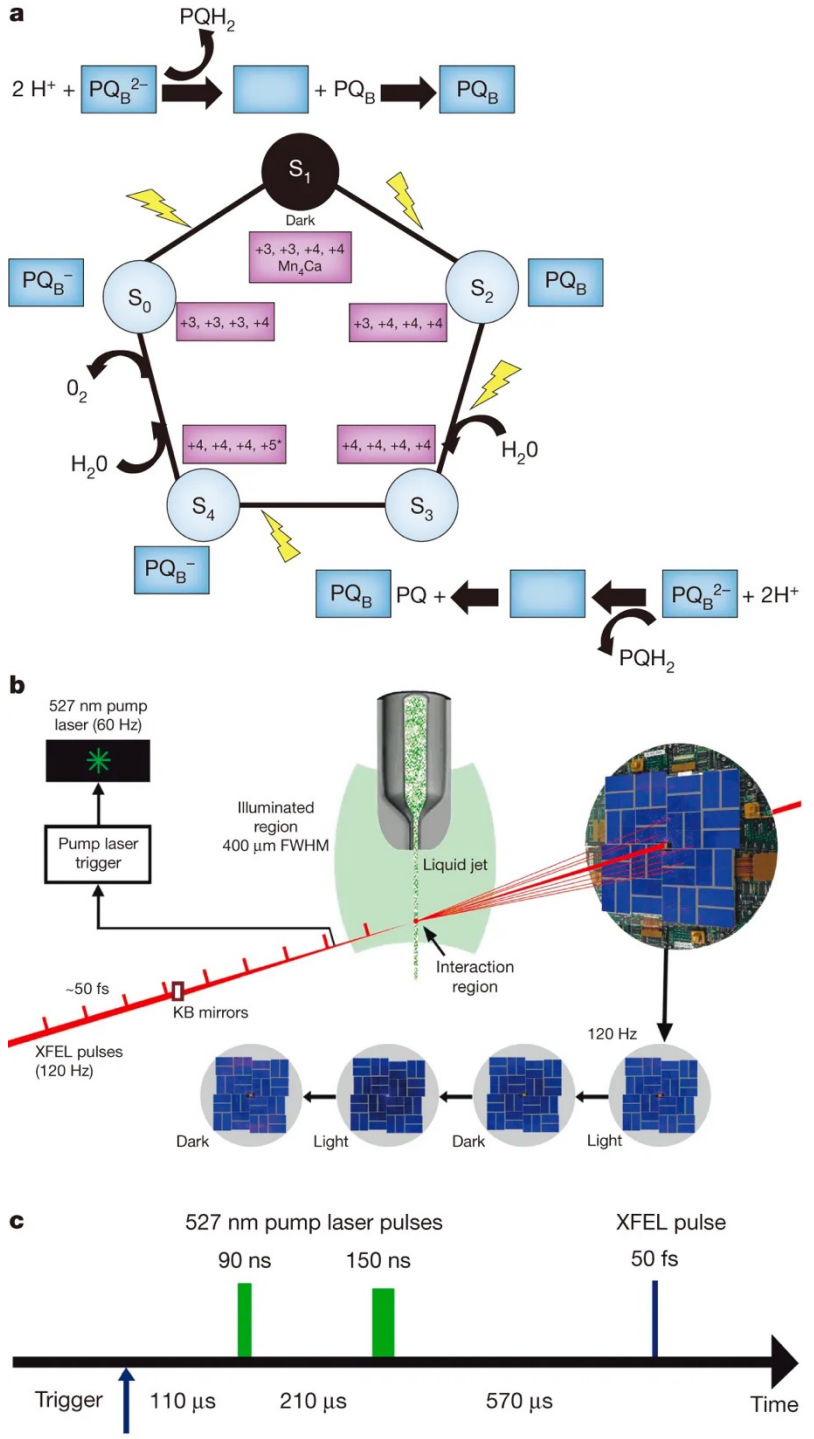

Recent results from SwissFEL

Article

Femtosecond-to-millisecond structural changes in a light-driven sodium pump

https://doi.org/10.1038/s41586-020-2307-8
Received: 29 November 2019
Accepted: 16 April 2020
Published online: 20 May 2020
Check for updates

Petr Skopintsev[1], David Ehrenberg[2,13], Tobias Weinert[1,13], Daniel James[1], Rajiv K. Kar[3], Philip J. M. Johnson[4], Dmitry Ozerov[5], Antonia Furrer[1], Isabelle Martiel[6], Florian Dworkowski[6], Karol Nass[6,7], Gregor Knopp[7], Claudio Cirelli[7], Christopher Arrell[8], Dardan Gashi[1,7], Sandra Mous[9], Maximilian Wranik[1], Thomas Gruhl[1], Demet Kekilli[1], Steffen Brünle[1], Xavier Deupi[1,10], Gebhard F. X. Schertler[1,11], Roger M. Benoit[1,12], Valerie Panneels[1], Przemyslaw Nogly[9], Igor Schapiro[3], Christopher Milne[7], Joachim Heberle[2] & Jörg Standfuss[1]✉

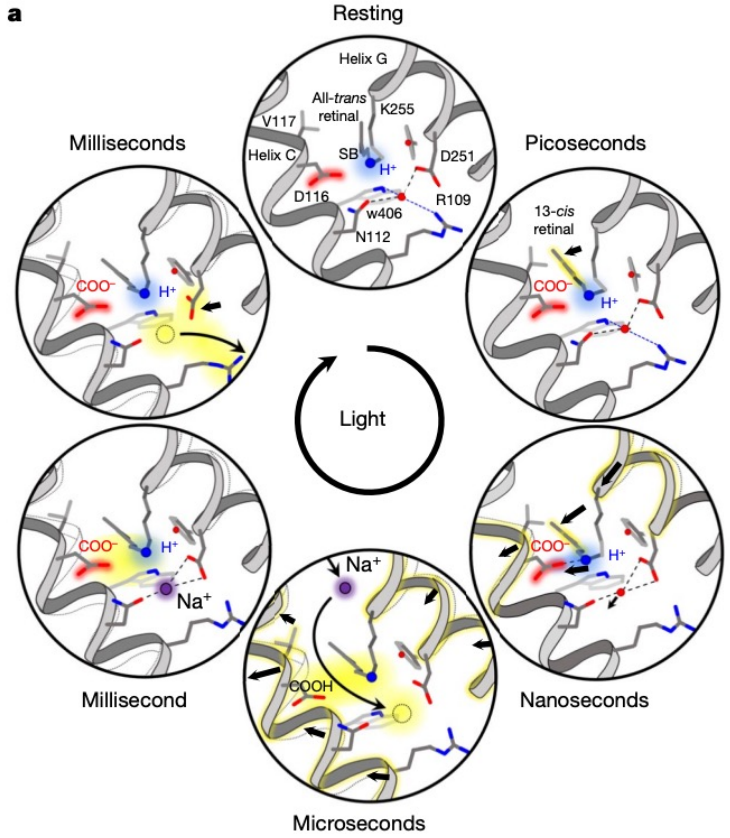

Light-driven sodium pumps actively transport small cations across cellular membranes[1]. These pumps are used by microorganisms to convert light into membrane potential and have become useful optogenetic tools with applications in neuroscience. Although the resting state structures of the prototypical sodium pump *Krokinobacter eikastus* rhodopsin 2 (KR2) have been solved[2,3], it is unclear how structural alterations over time allow sodium to be translocated against a concentration gradient. Here, using the Swiss X-ray Free Electron Laser[4], we have collected serial crystallographic data at ten pump–probe delays from femtoseconds to milliseconds. High-resolution structural snapshots throughout the KR2 photocycle show how retinal isomerization is completed on the femtosecond timescale and changes the local structure of the binding pocket in the early nanoseconds. Subsequent rearrangements and deprotonation of the retinal Schiff base open an electrostatic gate in microseconds. Structural and spectroscopic data, in combination with quantum chemical calculations, indicate that a sodium ion binds transiently close to the retinal within one millisecond. In the last structural intermediate, at 20 milliseconds after activation, we identified a potential second sodium-binding site close to the extracellular exit. These results provide direct molecular insight into the dynamics of active cation transport across biological membranes.

KR2 resting state

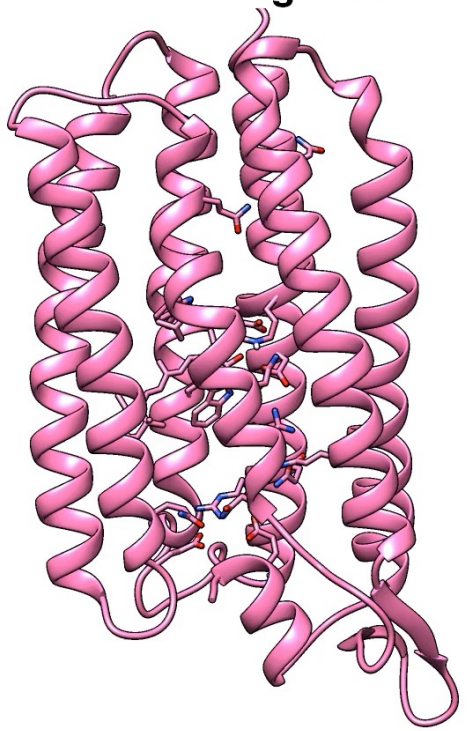

Some notes on X-ray Spectroscopy

Remember: interaction of x-rays with matter

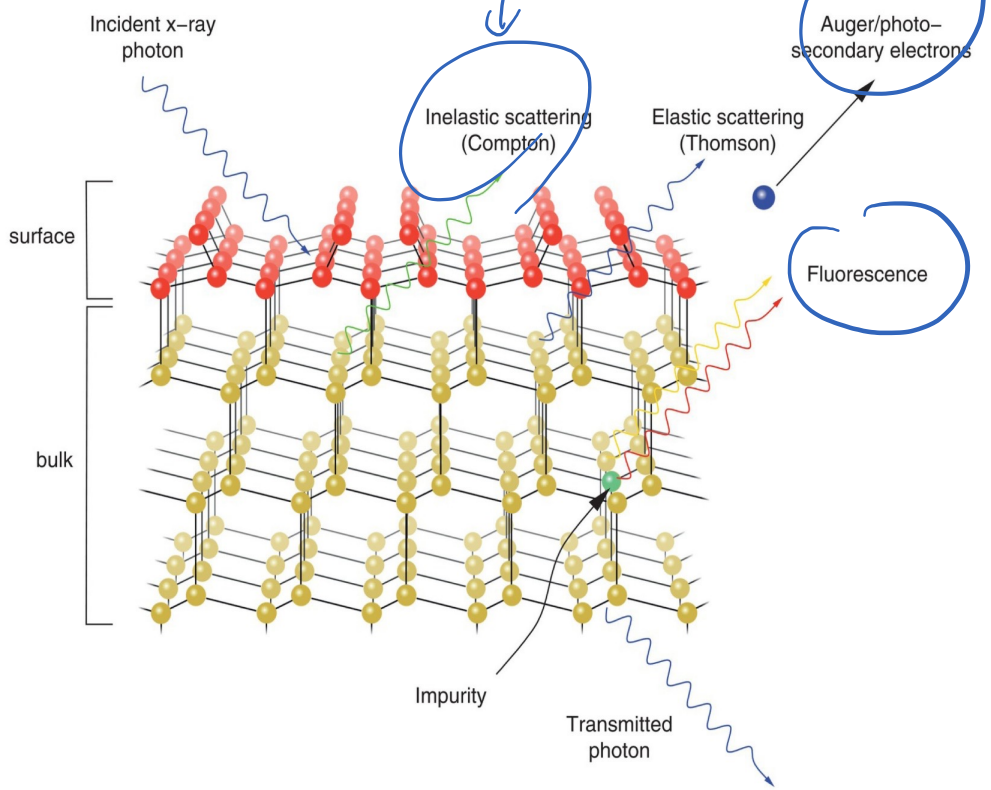

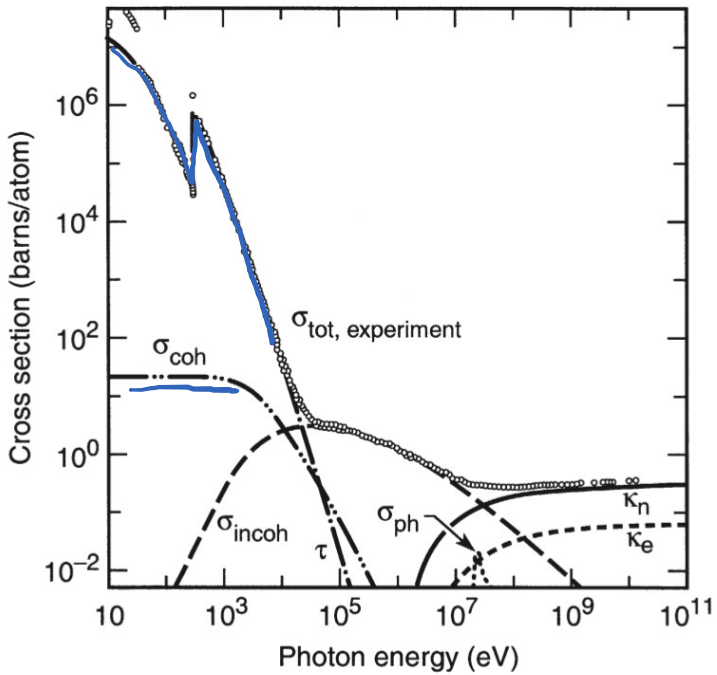

Fig. 3-1. Total photon cross section σ_{tot} in carbon, as a

Photoionization / absorption

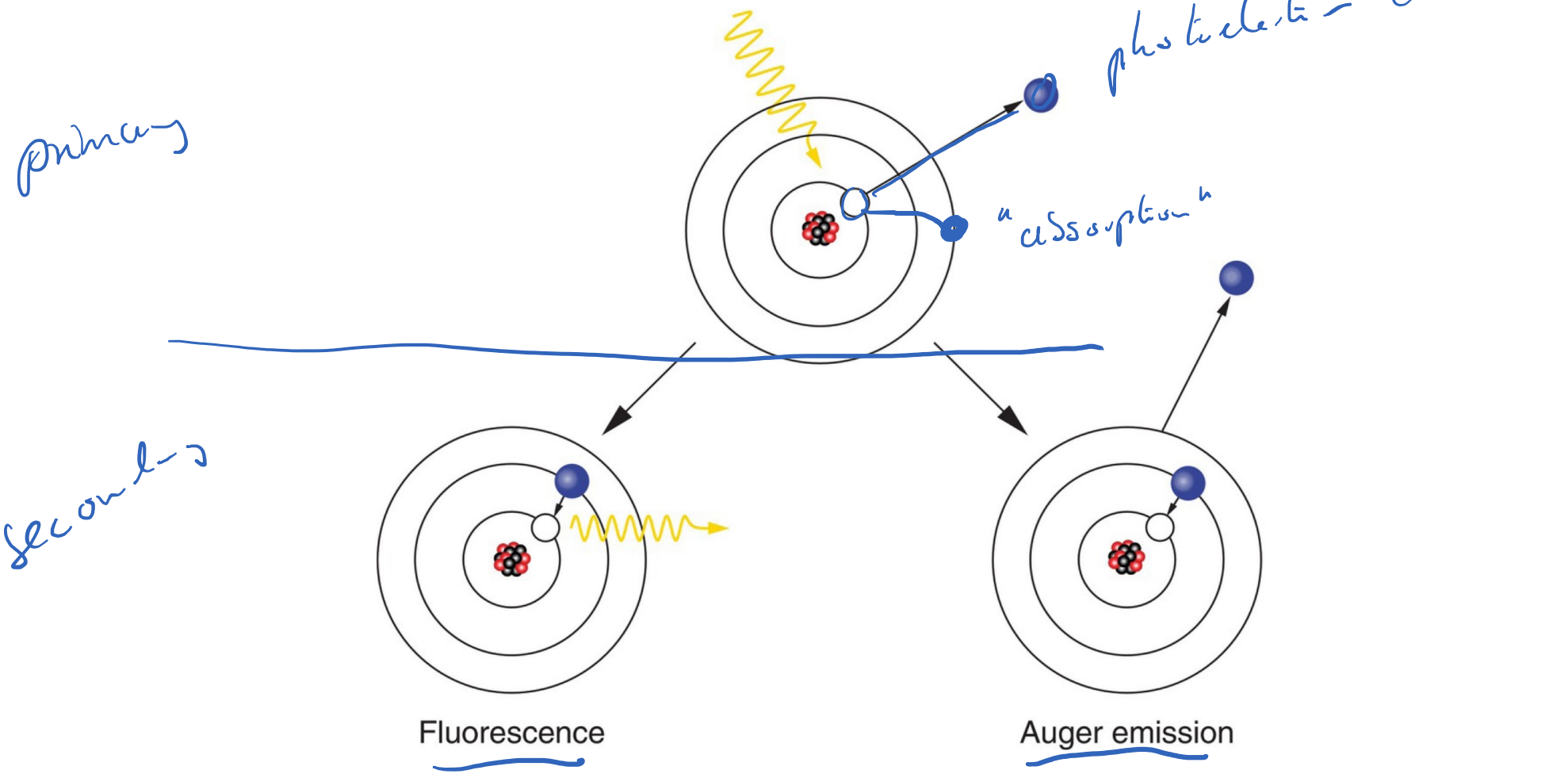

Atoms vs molecules → Core level spectroscopy

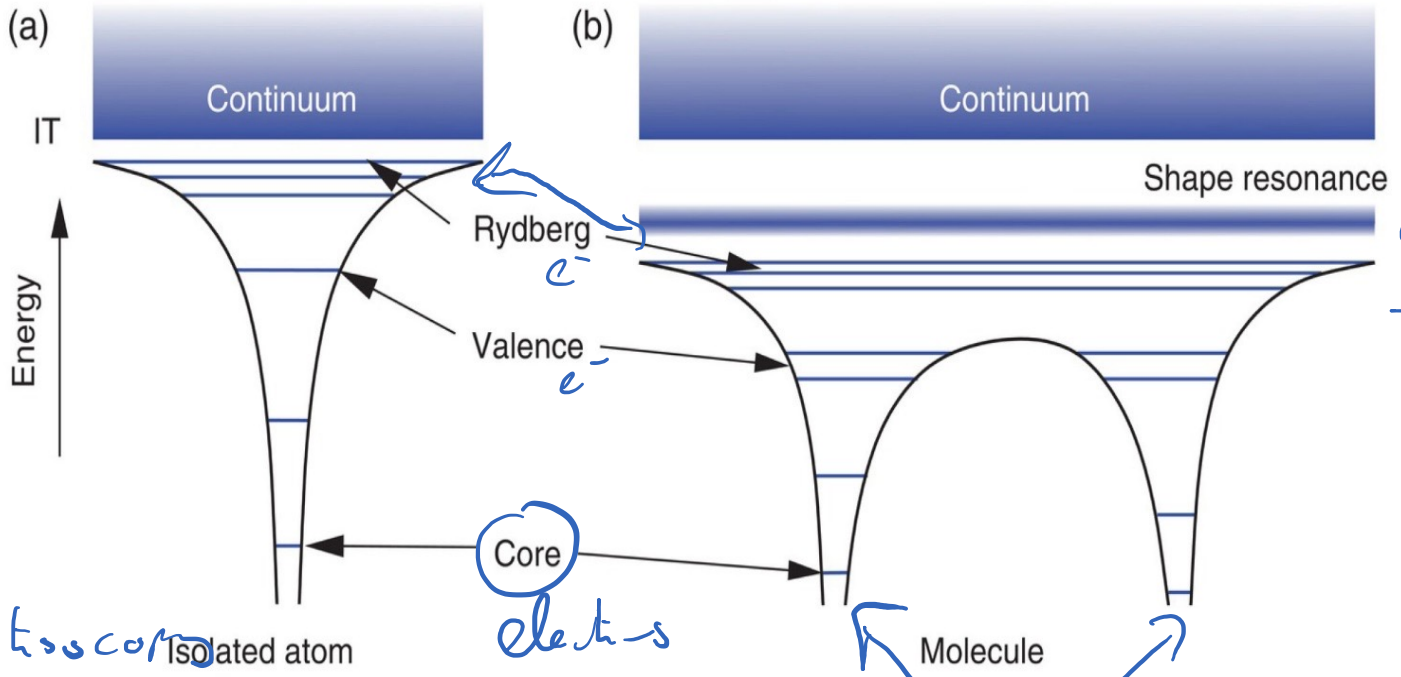

empty states

chemistry in empty states

Core binding

of

core electrons

of

chemical shifts

x-ray spectroscopy

① element specific

② sensitive to local electron density

different for different chemistry

Absorption vs Photoemission

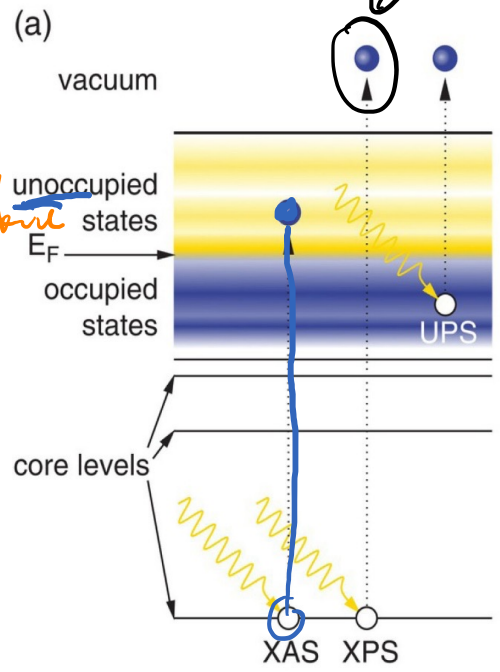

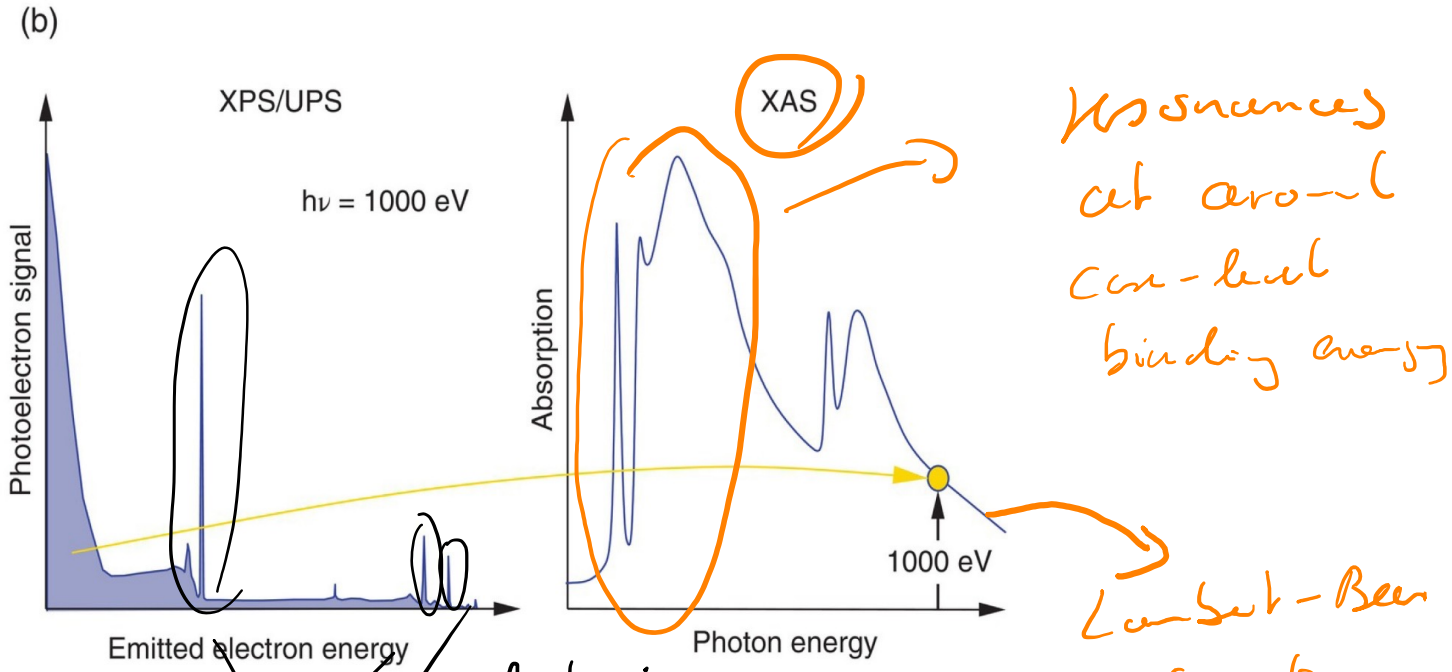

Photoemission:

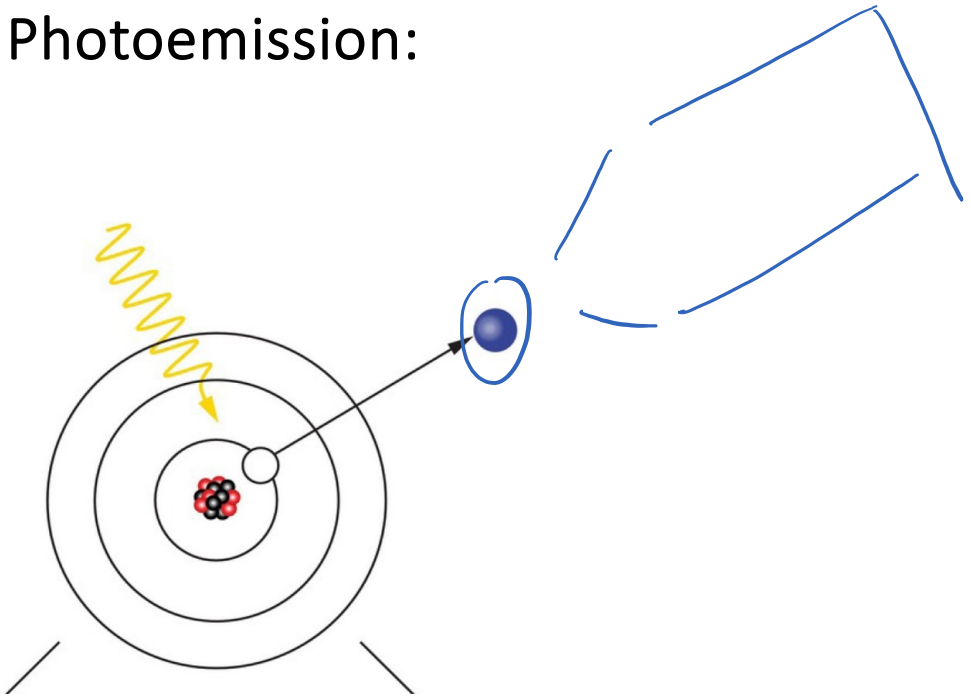

→ Electron kinetic energy analyzer

$$M + h\nu \rightarrow M^+ + e^-$$

$$E_{kin} = h\nu - E_B - e\phi$$

E_B: binding energy

ϕ: work function

Note put e^- into continuum of states

how all states infinitely close

→ all transitions are allowed

Photoelectrons reflect occupied density of states

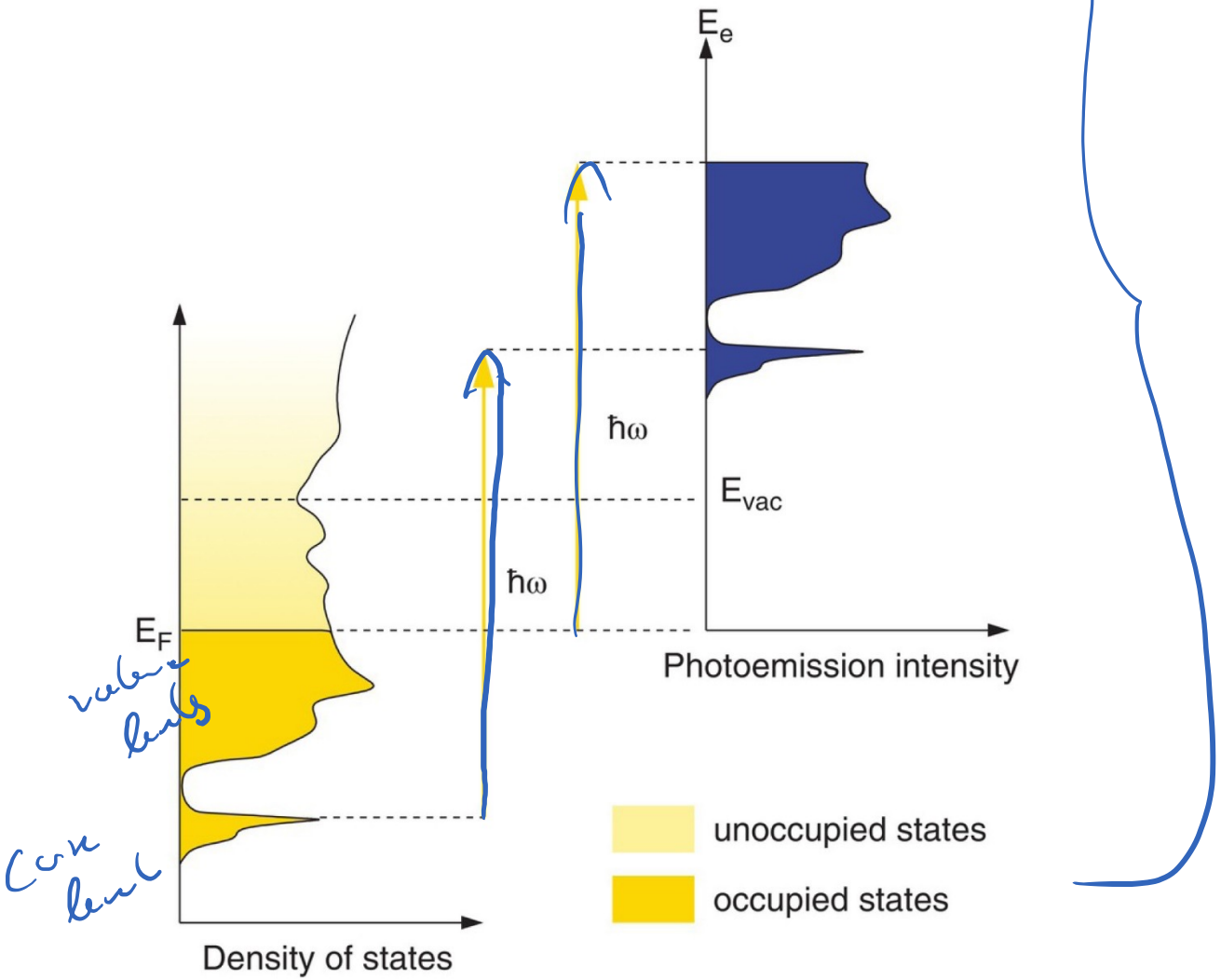

The interpretation of photoelectron-spectroscopy (PES, XPS) is that for a fixed $h\nu$ the photo-emission intensity reflects the density of occupied states

Ionization energies of elements → Session 1

Table 1-1. Electron binding energies, in electron volts, for the elements in their natural forms.

Element	K 1s	L_1 2s	L_2 $2p_{1/2}$	L_3 $2p_{3/2}$	M_1 3s	M_2 $3p_{1/2}$	M_3 $3p_{3/2}$	M_4 $3d_{3/2}$	M_5 $3d_{5/2}$	N_1 4s	N_2 $4p_{1/2}$
1 H	13.6										
2 He	24.6*										
3 Li	54.7*										
4 Be	111.5*										
5 B	188*										
6 C	284.2*										
7 N	409.9*	37.3*									
8 O	543.1*	41.6*									
9 F	696.7*										
10 Ne	870.2*	48.5*	21.7*	21.6*							
11 Na	1070.8†	63.5†	30.65	30.81							
12 Mg	1303.0†	88.7	49.78	49.50							
13 Al	1559.6	117.8	72.95	72.55							
14 Si	1839	149.7*b	99.82	99.42							
15 P	2145.5	189*	136*	135*							
16 S	2472	230.9	163.6*	162.5*							
17 Cl	2822.4	270*	202*	200*							
18 Ar	3205.9*	326.3*	250.6†	248.4*	29.3*	15.9*	15.7*				
19 K	3608.4*	378.6*	297.3*	294.6*	34.8*	18.3*	18.3*				
20 Ca	4038.5*	438.4†	349.7†	346.2†	44.3 †	25.4†	25.4†				
21 Sc	4492	498.0*	403.6*	398.7*	51.1*	28.3*	28.3*				
22 Ti	4966	560.9†	460.2†	453.8†	58.7†	32.6†	32.6†				

Each element has a characteristic binding energy or electronic structure

⇒ use XPS for chemical analysis

E.g. $h\nu = 700$ eV you see peaks at ~160 eV, 420 eV

↓ O, ↓ C

Chemical shifts

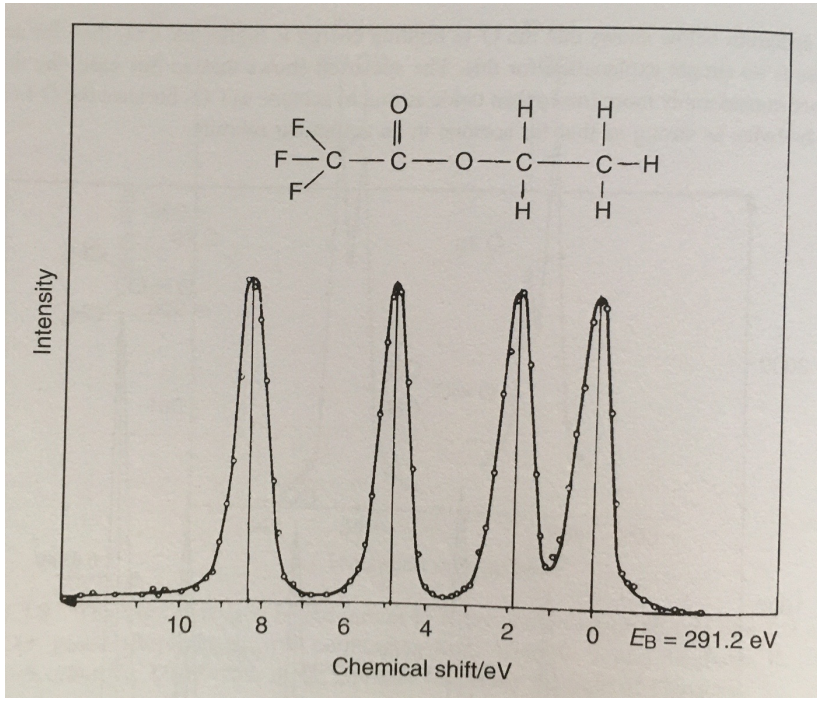

High resolution XPS can yield information about binding configuration / chemical environment of target atom

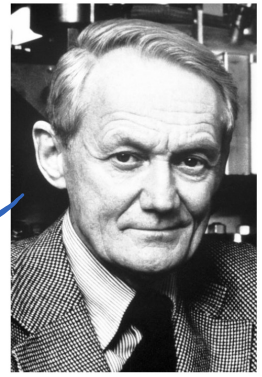

Photo from the Nobel Foundation archive.
Kai M. Siegbahn
Prize share: 1/2

different oxidation states lead to characteristic shift of the core level binding energies [chemical shifts]

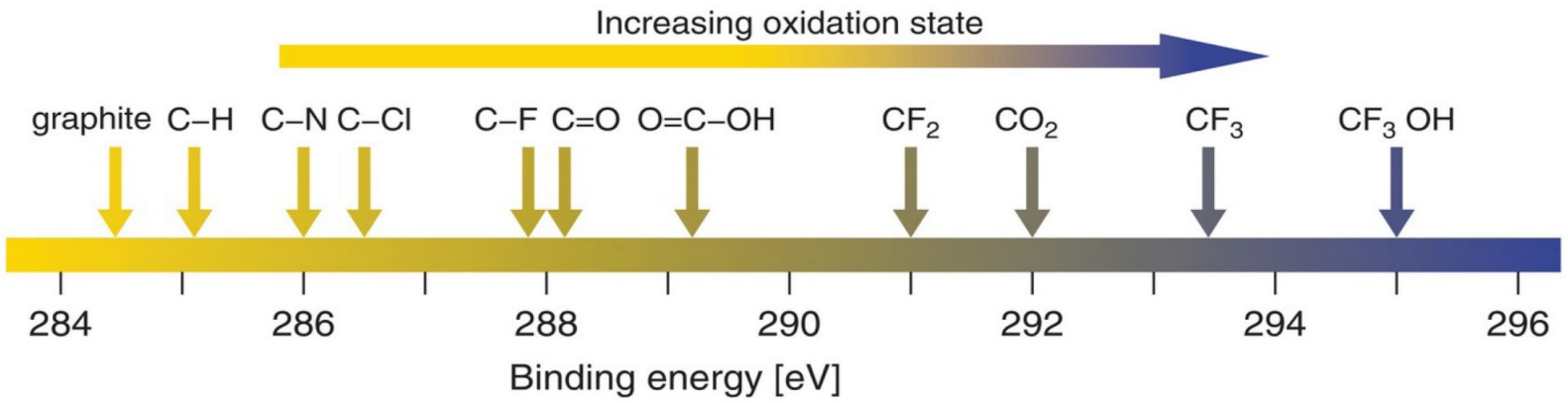

Generally

higher oxidation states lead to large chemical shifts

Vibrational information in photoelectron spectroscopy

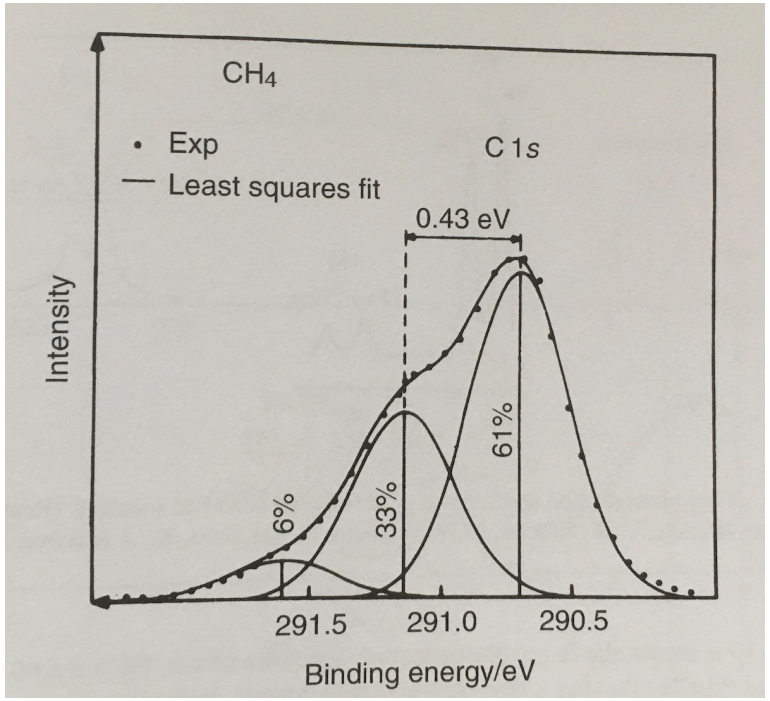

Brief comment

Core level binding energies

can even reflect vibrational levels

The „universal curve of photoemission“

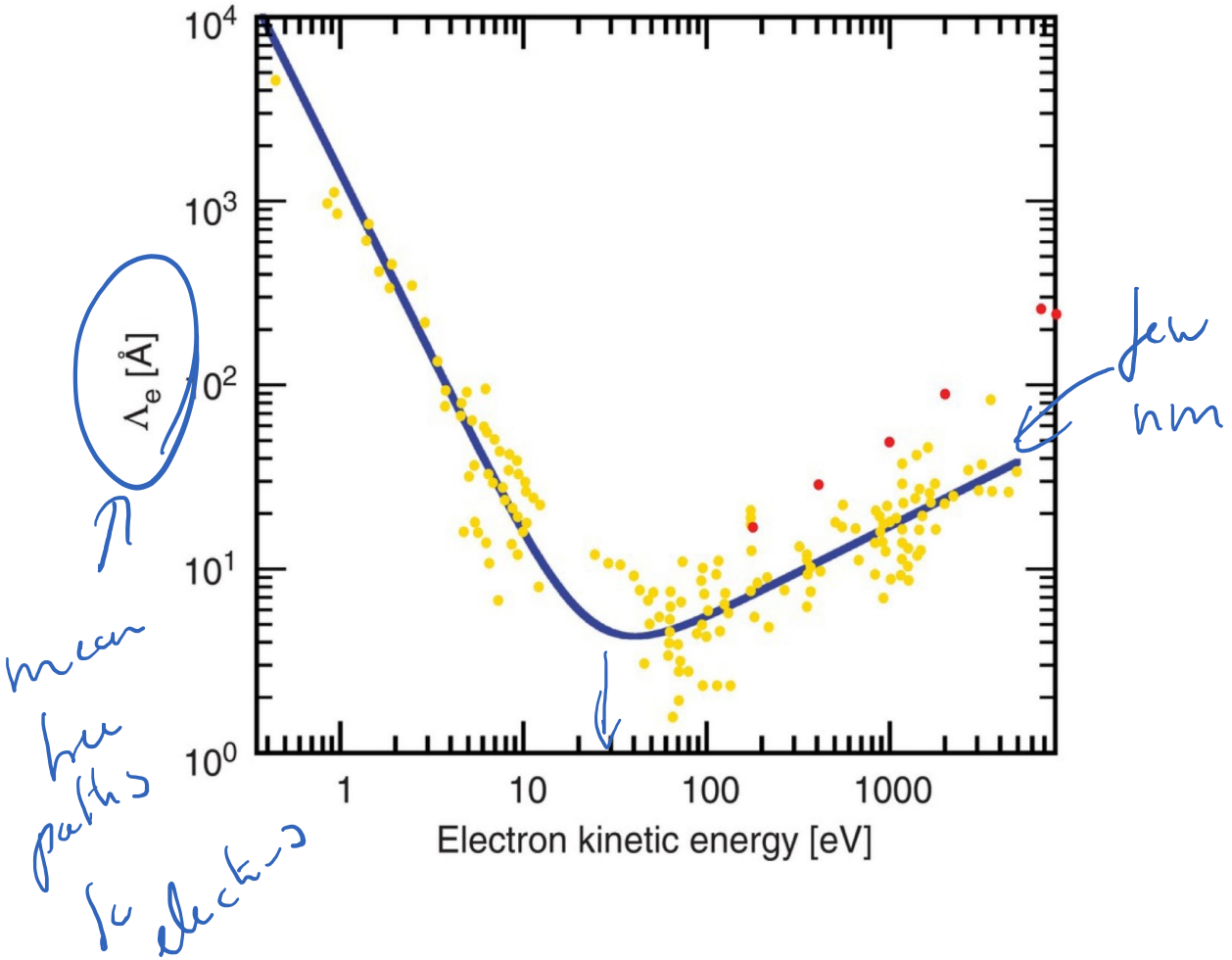

→ (photo) electrons are scattered in any material

→ escape depths depends on kinetic energy

→ overall surface sensitive technique

X-ray absorption XAS

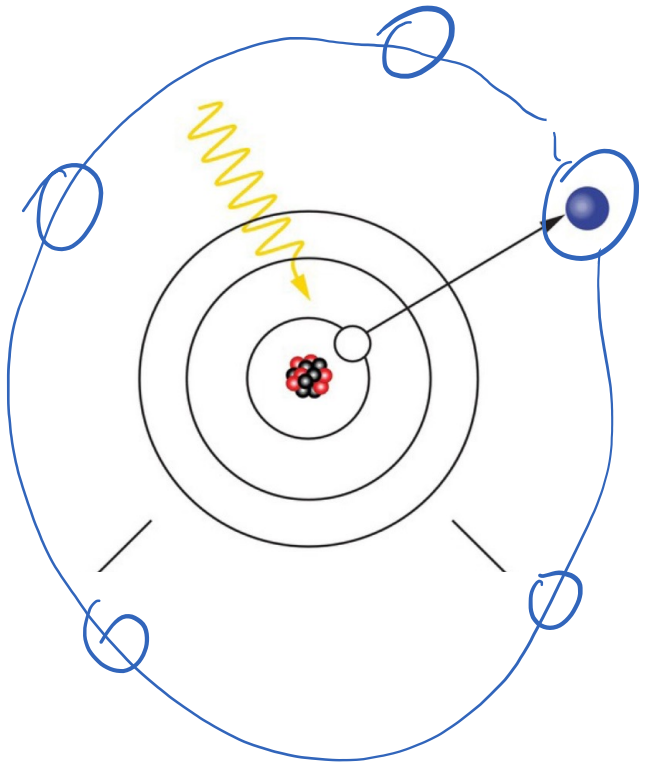

→ promote electron into specific states

→ highly sensitive to (dipole) selection rules

$l \pm 1$

→ Fermi Golden Rule

$$\Gamma_{ij} = \frac{2\pi}{\hbar} |\langle f|H|i\rangle|^2 \mathcal{E}$$

⇒ probing partial density of states

Table 1-1. Electron binding energies, in electron volts, for the elements in their natural forms.

Element	K 1s	L_1 2s	L_2 $2p_{1/2}$	L_3 $2p_{3/2}$	M_1 3s	M_2 $3p_{1/2}$	M_3 $3p_{3/2}$	M_4 $3d_{3/2}$	M_5 $3d_{5/2}$	N_1 4s	N_2 $4p_{1/2}$
1 H	13.6										
2 He	24.6*										
3 Li	54.7*										
4 Be	111.5*										
5 B	188*										
6 C	284.2*										
7 N	409.9*	37.3*									
8 O	543.1*	41.6*									
9 F	696.7*										
10 Ne	870.2*	48.5*	21.7*	21.6*							
11 Na	1070.8†	63.5†	30.65	30.81							
12 Mg	1303.0†	88.7	49.78	49.50							
13 Al	1559.6	117.8	72.95	72.55							
14 Si	1839	149.7*b	99.82	99.42							
15 P	2145.5	189*	136*	135*							
16 S	2472	230.9	163.6*	162.5*							
17 Cl	2822.4	270*	202*	200*							
18 Ar	3205.9*	326.3*	250.6†	248.4*	29.3*	15.9*	15.7*				
19 K	3608.4*	378.6*	297.3*	294.6*	34.8*	18.3*	18.3*				
20 Ca	4038.5*	438.4†	349.7†	346.2†	44.3 †	25.4†	25.4†				
21 Sc	4492	498.0*	403.6*	398.7*	51.1*	28.3*	28.3*				
22 Ti	4966	560.9†	460.2†	453.8†	58.7†	32.6†	32.6†				

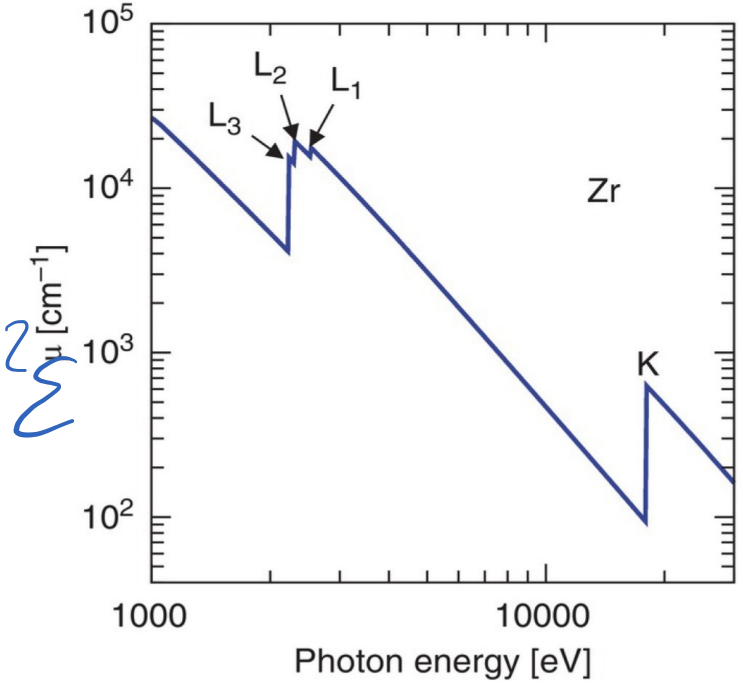

Distinct regions of X-ray absorption

XANES
x-ray absorption near edge structure
↳ direct measurement / sensitive to empty states (LUMO)
↓
local electronic structure

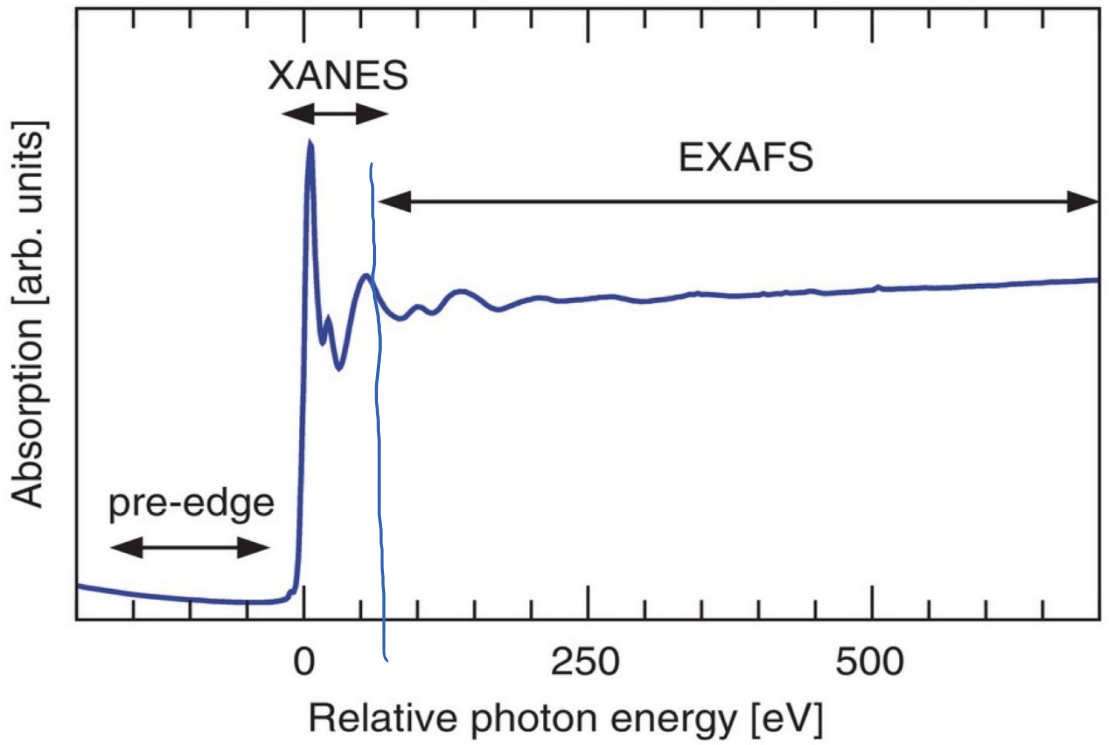

X-ray Absorption Near Edge Structure (XANES)

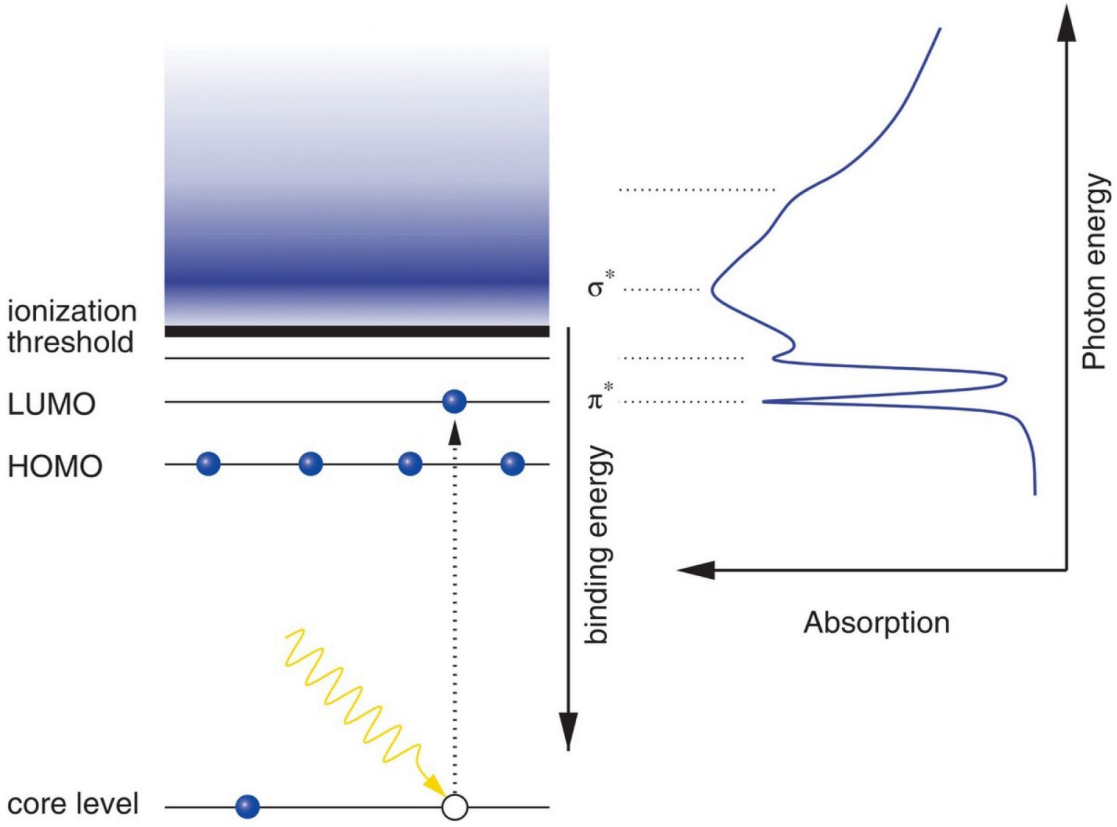

→ probe unoccupied states

→ probe local electronic structure

→ conclusions about local binding environment

XANES spectra yield detailed information about bonding structure

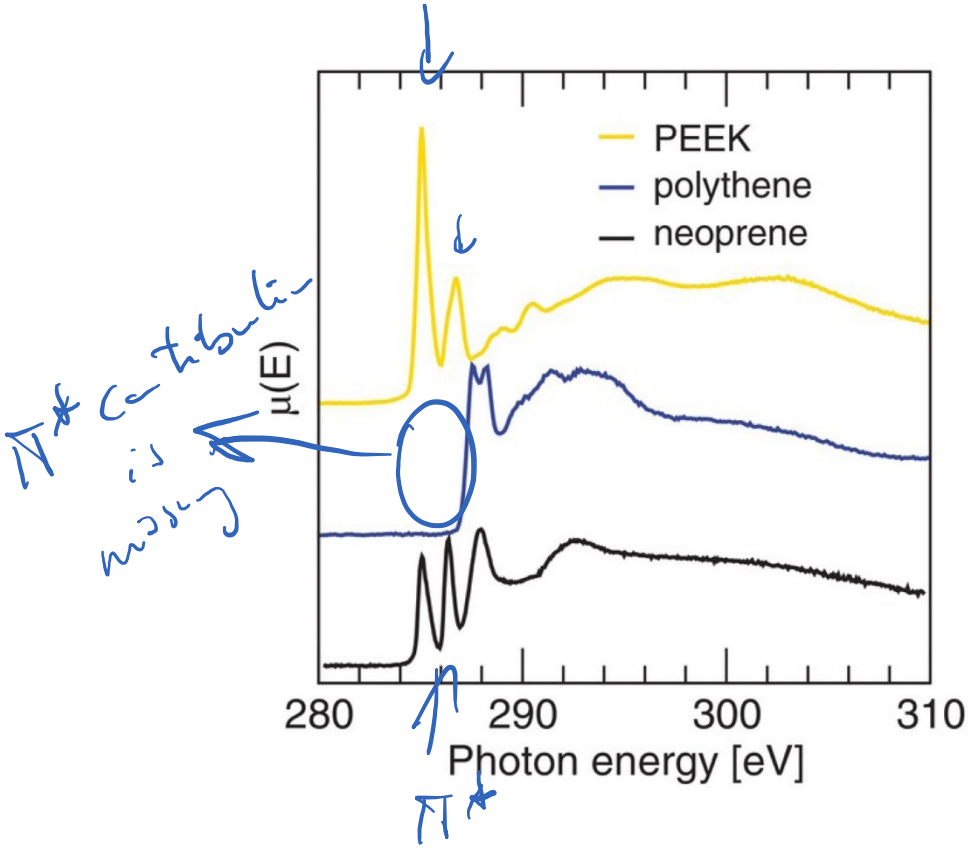

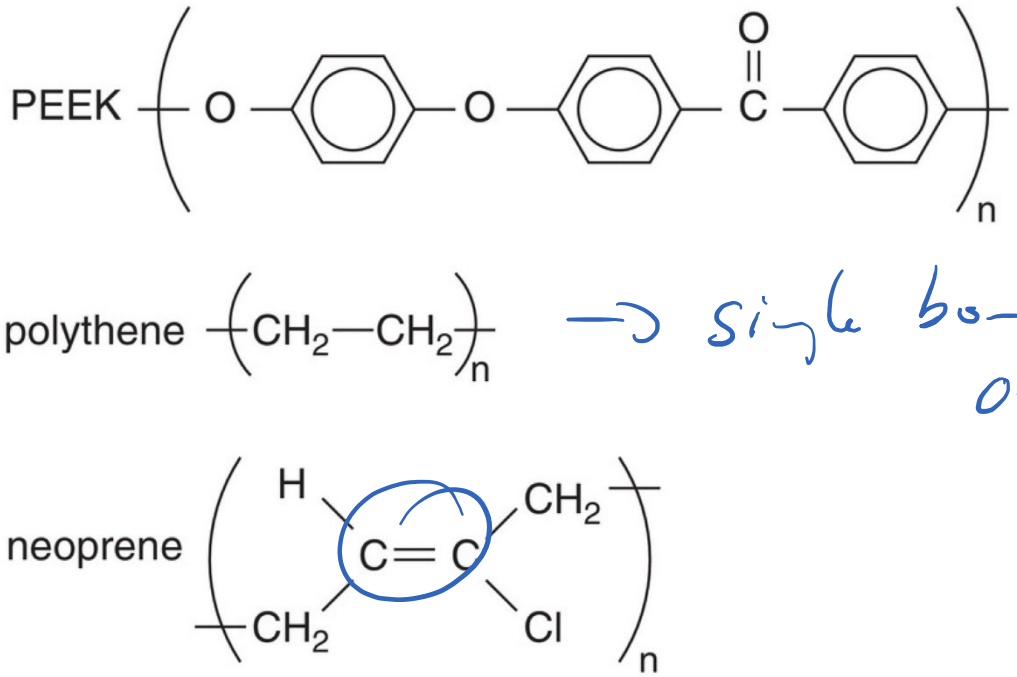

Extended X-ray Absorption Fine Structure (EXAFS) contains information about nearest neighbors

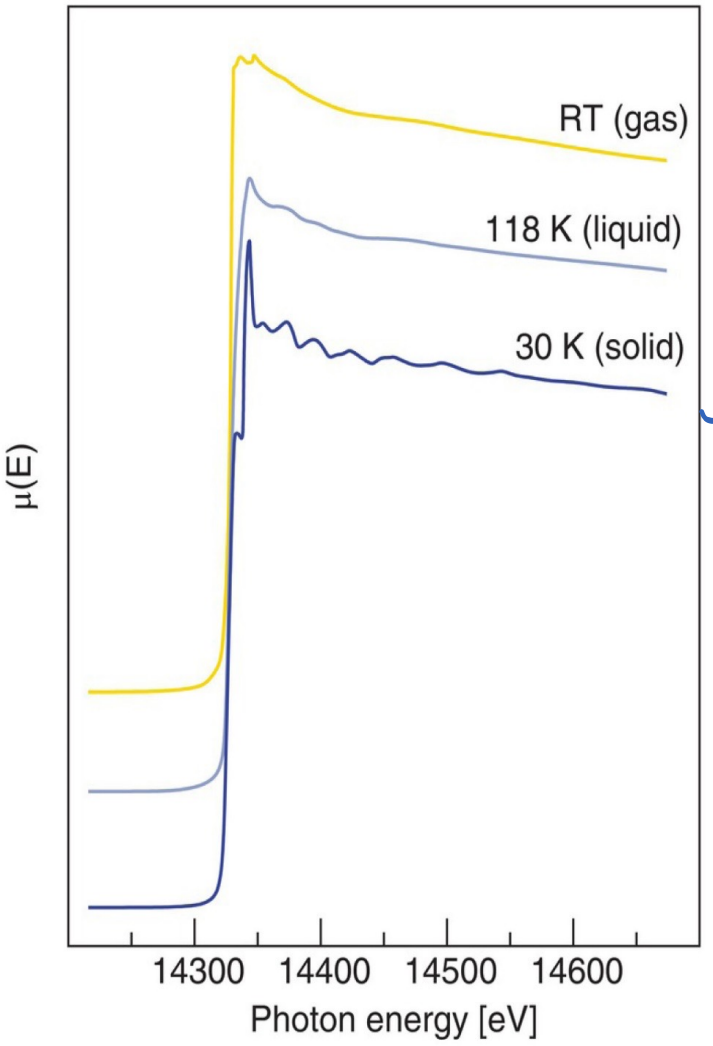

Wiggles for (slow) electrons just beyond IP

→ effects from nearest neighbors

⇒ these distinct phases of the same sample lead to distinct absorption fine structure beyond IP

EXAFS and nearest neighbors

Remarks

particle wave duality

⇓

electron with E_{kin} have an associated wavelength $\lambda = \frac{h}{mc}$

⇒ can scatter like a wave

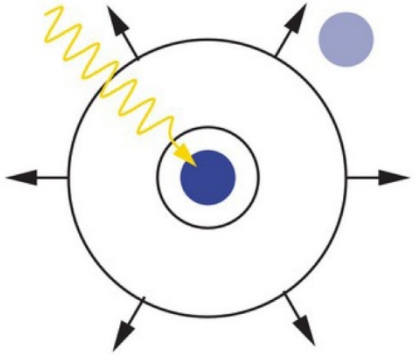

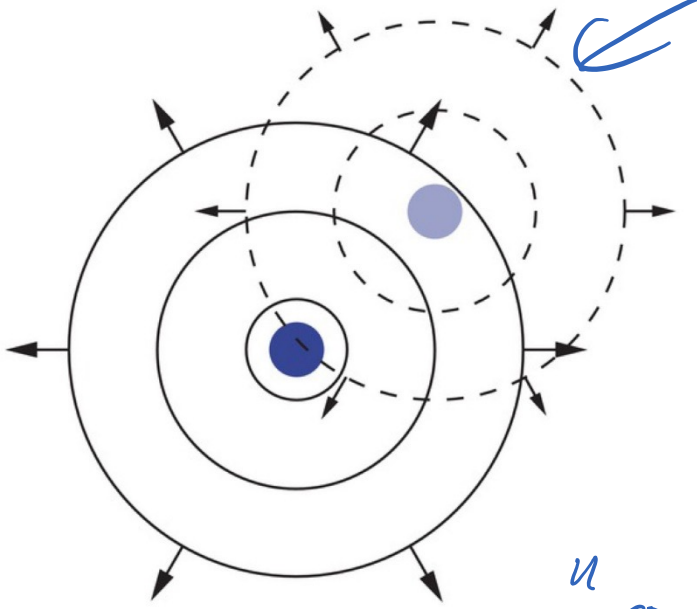

interference phenomena from neighbors

⇓

Ripples

"outgoing electrons can scatter at neighboring atoms"

EXAFS interference examples

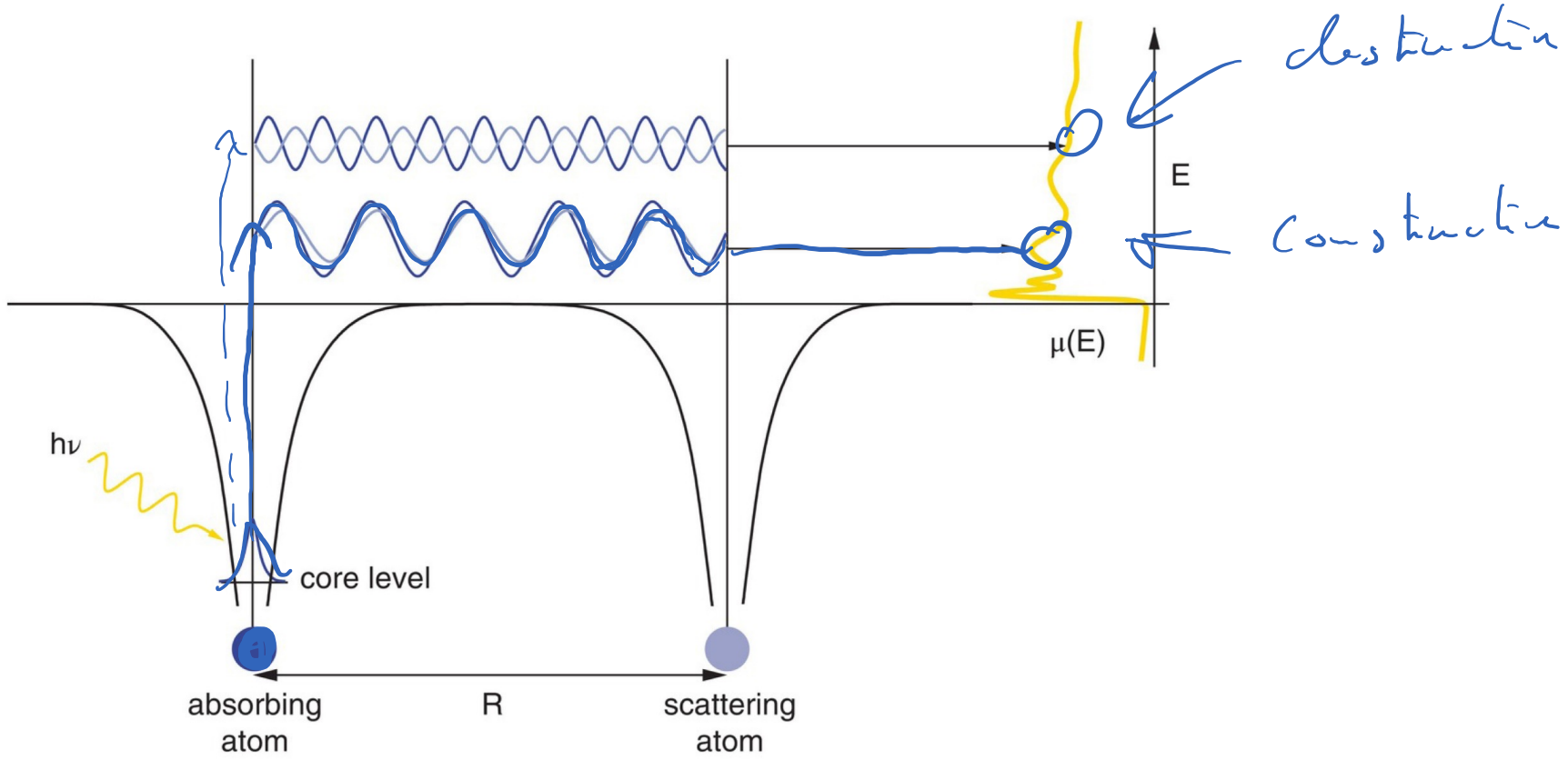

Characteristic features in EXAFS → rules of thumb

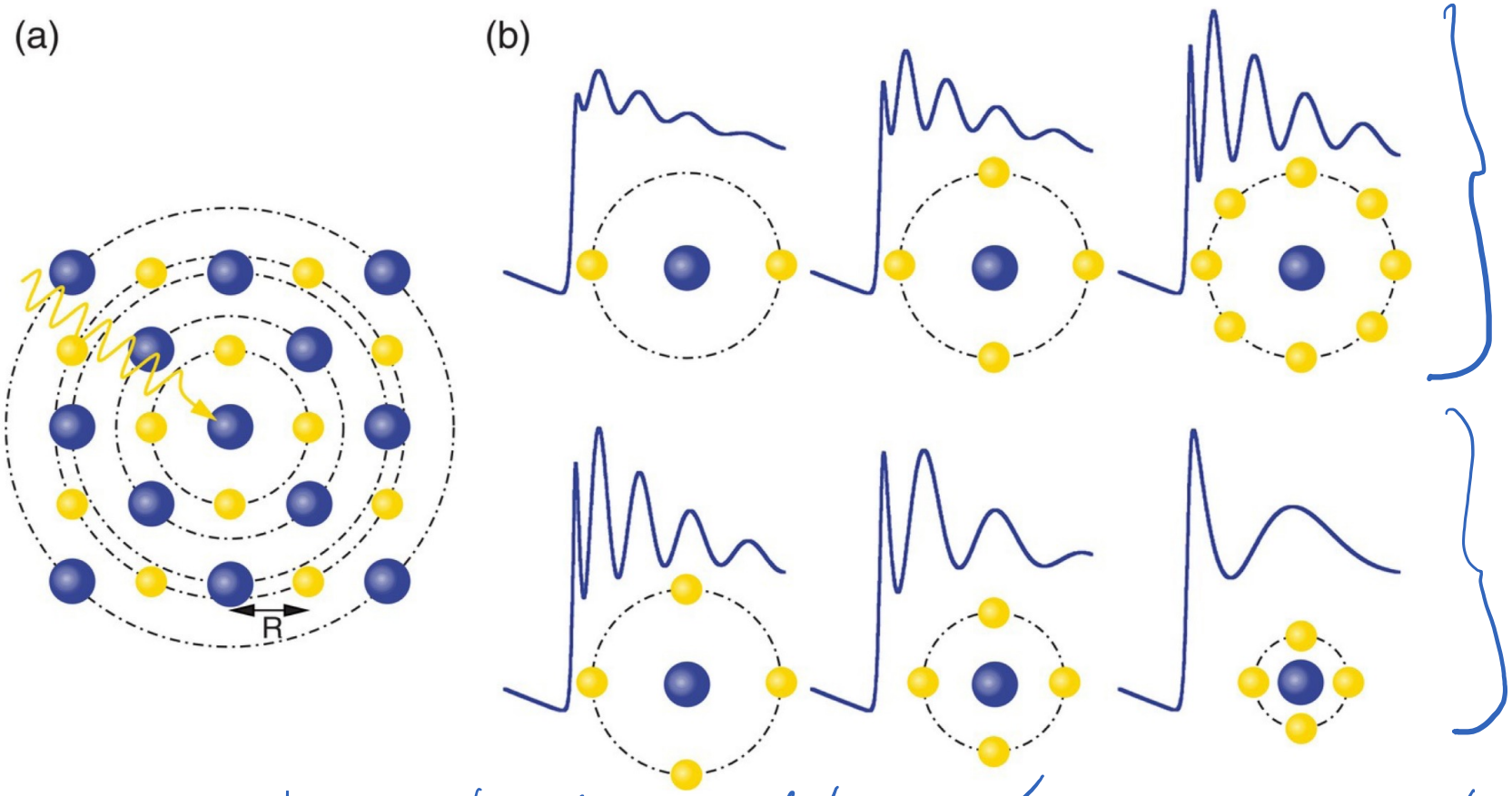

oscillation signal increases with number of neighbors

depends on shell size

Generally theoretical modelling / comparison to reference spectra for data analysis

The end